

Role of Lamin A and Telomerase in DNA Damage Response



A thesis submitted towards partial fulfillment of
BS MS Dual Degree programme

By

Sishil Sushanth

20111026

Dr. Kundan Sengupta

(Assistant Professor, IISER Pune & Wellcome-Trust DBT India Alliance Intermediate Fellow)

**Chromosome Biology Lab
Indian Institute of Science Education and Research (IISER) Pune**

Certificate

This is to certify that this dissertation entitled “Role of Lamin A and Telomerase in DNA Damage Response” towards the partial fulfillment of the BS-MS dual degree programme at the Indian Institute of Science Education and Research (IISER) Pune, represents original research carried out by Sishil Sushanth at CHROMOSOME BIOLOGY LAB (CBL), IISER Pune under the supervision of Dr. Kundan Sengupta, Assistant Professor, IISER Pune during the academic year 2015-2016.



Dr. Kundan Sengupta
Assistant Professor
Department of Biology, IISER PUNE

Date: 28.03.2016

Declaration

I hereby declare that all the matter embodied in the report entitled “Role of Lamin A and Telomerase in DNA Damage Response” are the results of the investigations carried out by me at the Department of Biology, Indian Institute of Science Education and Research (IISER) Pune, under the supervision of Dr. Kundan Sengupta, Assistant Professor, IISER Pune and the same has not been submitted anywhere else for any other degree.



Sishil Sushanth
20111026
BS-MS student
IISER PUNE

Date: 28.03.2016

Abstract

Lamins are intermediate filament proteins that maintain structural and mechanical integrity of the nucleus. Lamins are important in maintenance of the epigenetic landscape, DNA replication and mechanotransduction. Lamins have also been implicated in DNA damage response. Telomerase – a reverse transcriptase enzyme expressed in germ cells and deregulated in cancers, protects transformed cells against DNA damage. In this study, we attempted to understand the coregulatory role of Lamin A and Telomerase in DNA Damage response. Down regulation of Lamin A using shRNA in HT1080 (Telomerase positive) and U2OS (Telomerase negative) cells led to significant decrease in 53BP1 (a key regulator of NHEJ mediated DNA damage repair pathway) foci volumes and changes in foci numbers upon DNA damage induction using Cisplatin. Lamin A downregulated cells showed an enrichment of the 53BP1 foci at the nuclear periphery. HT1080 cells stably overexpressing Telomerase showed comparable levels of basal DNA damage despite being aneuploid and displayed significant downregulation of B-type Lamins. This data suggests a potential cross talk between Telomerase and Lamins in regulating DNA damage response.

INDEX

| | |
|------------------------------------|----|
| 1. Certificate..... | 1 |
| 2. Declaration..... | 2 |
| 3. Abstract..... | 3 |
| 4. List of Figures and Tables..... | 5 |
| 5. Acknowledgement..... | 6 |
| 6. Introduction..... | 7 |
| 7. Materials and Methods..... | 13 |
| 8. Results..... | 24 |
| 9. Discussion..... | 45 |
| 10. Future Directions..... | 53 |
| 11. Reference..... | 54 |

List of Figure and Tables

| | |
|--|----|
| Figure 1.1: Structure of Mammalian Telomeres..... | 7 |
| Figure 1.2: Factors involved in DNA Damage response in Mammals and Yeast..... | 9 |
| Figure 1.3: Domain organization of Telomerase enzyme..... | 9 |
| Figure 1.4: Role of Lamin A in DNA damage response pathways..... | 10 |
| Figure 2.1: Levels of Lamins, hTERT and 53BP1 in HT1080, ST-HT1080 and U2OS cells..... | 24 |
| Figure 2.2: Transcript levels of Lamins and hTERT in HT1080, ST-HT1080 and U2OS cells..... | 25 |
| Figure 2.3: Transcript levels of Lamins and hTERT across cancer cell lines..... | 26 |
| Figure 2.4: Transcript levels of Lamins upon hTERT overexpression in HT1080 and U2OS cells..... | 28 |
| Figure 2.5: ALT associated PML bodies in U2OS cells upon hTERT overexpression | 29 |
| Figure 2.6: Ploidy levels in HT1080, ST-HT1080 and U2OS cells..... | 30 |
| Figure 2.7: Telomere status in HT1080, ST-HT1080 and U2OS cells..... | 31 |
| Figure 2.8: Basal level of DNA damage in HT1080 and ST-HT1080 cells..... | 32 |
| Figure 2.9: Cisplatin dose response in HT1080 and ST-HT1080 cells..... | 33 |
| Figure 2.10: Cisplatin dose response in Lamin A downregulated HT1080 cells..... | 35 |
| Figure 2.11: Cisplatin dose response in Lamin A downregulated U2OS cells..... | 37 |
| Figure 2.12: 53BP1 volume distribution in Lamin A downregulated cells..... | 40 |
| Figure 2.13: Median distance measurements of 53BP1 foci from the nuclear periphery in Lamin A downregulated cells..... | 42 |
| Figure 2.14: hTERT versus Lamin levels across Cancers..... | 44 |
| Figure 2.14: hTERT versus 53BP1, DNA-PKcs, KU70-80 levels across Cancers..... | 44 |
| Figure 3.1: Transcription factor overlap between Lamin promoters..... | 50 |
| Figure 3.2: Model depicting the observations and the pathway emerging from the study..... | 52 |

Acknowledgement

I express my sincere gratitude to Dr. Kundan Sengupta, Assistant Professor, Chromosome Biology Lab, Indian Institute of Science Education and Research (IISER) Pune, for his valuable guidance and letting me work in his lab. I would also like to thank him for encouraging and allowing me to try to test out my own ideas and experiments during the study.

I would like to thank Roopali for her immense amount of patience and guidance without which I would not have completed the project.

I convey my gratitude to all CBL lab members for their constant support and guidance.

I thank IISER Pune for providing excellent facilities as well as exposure to science,

INTRODUCTION

The DNA regulates cell function. The nucleus has two major components, the (i) nuclear envelope and (ii) the nucleoplasm in which the chromatin is present in highly organized structures and acquires a non-random position inside the nucleus (Cremer et al., 2001). Compared to bacteria, which have a circular chromosome, the mammalian chromosomes are linear, whose ends are protected from DNA damage by Telomeres. Telomeres are nucleoprotein structures characterized by the presence of tandem TTAGGG repeats and helps in distinguishing chromosomal ends from DNA breaks (Doksani and de Lange, 2014). Thus, Telomeres prevents chromosomes from fusing with one another and there by play a pivotal role in maintaining genome integrity (Fig 1.1).

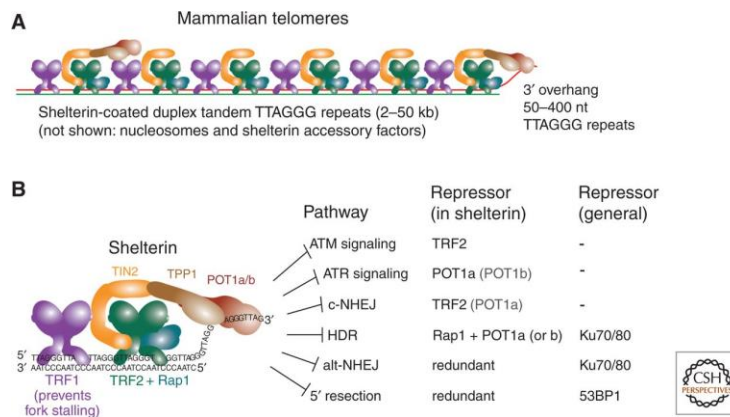


Figure 1.1: (A) The structure of Mammalian Telomeres bound by Shelterin complex. (B) Schematic representing the Shelterin subunits that inhibit the pathways that regulate chromosomal end protection. Adapted from Doksani and de Lange, 2014.

Telomeres act as buffers at the ends of chromosome which shorten during cell division and the multiprotein complex - Shelterin, protects these repeats and has crucial roles in telomere length regulation and protecting chromosomal ends. Shelterin is a telomere specific complex consisting of six components - TRF1 (Telomeric Repeat Factor 1), TRF2 (Telomere Repeat Factor 2), POT1 (Protection of Telomeres 1), TIN2 (TRF1 and TRF2 Interacting Nuclear Protein 2), TPP1 and RAP1 (Repressor/Activator Protein 1). TRF1 and TRF2 are homodimeric proteins that bind to double strand Telomere repeats

with the help of Myb/SANT-type binding domain that gives shelterin its specificity towards telomeres (Court et al., 2005). POT1, the third DNA binding component of shelterin, binds to single strand TTAGGG repeats with the help of two oligosaccharide/oligonucleotide binding (OB) folds. TPP1, which also contains the OB fold helps in the recruitment as well as binding of POT1. TPP1 also binds to TIN2 which itself associates with both TRF1 and TRF2 (Ye et al., 2004). TIN2 is essential for TRF1, TRF2 stabilization on telomeric DNA and helps in the recruitment of TPP1 and POT1. Rap1 interacts only with TRF2 and has a role in transcriptional regulation. Shelterin also helps in Telomerase recruitment and thus helps in the maintenance as well as telomere length homeostasis (Nandakumar et al., 2012).

Unprotected chromosomal ends trigger genomic instability that can be oncogenic. Telomere ends are kept under check by TRF2 and POT1 and thus suppress DNA damage signaling. Shelterin protects linear ends from DNA repair and degradation pathways, which includes - DNA damage signaling pathways mediated by ATM (ataxia telangiectasia mutated), ATR (ataxia telangiectasia and RAD3 related kinases) and double strand break (DSB) repair pathways mediated by non-homologous end joining (NHEJ) and homology directed repair (HDR). Shelterin also protects the chromosome ends from micro-homology mediated alternative-NHEJ and 5' Resection (Sfeir and de Lange, 2012) (Fig 1.1). The DNA damage-signaling pathway consists of carefully orchestrated cascade interactions of proteins required for the recognition, processing and elimination of the damaged region. Cells rely on either NHEJ or HR to carry out the repair process. NHEJ is opted throughout the cell cycle and is an error prone repair which involves processing of the DSB's followed by ligation (Lieber, 2010). In contrast, HR pathway involves a homologous template for the repair and is active during S and G2 phases of the cell cycle. Unlike NHEJ, HR pathway requires the resection of the DSB's and hence this step is the determining phase for the choice of pathways (Symington and Gautier, 2011). In addition p53-binding protein (53BP1) also regulates pathway choice by inhibiting resection and promoting NHEJ (Bothmer et al., 2011). The MRE11-RAD50-NBS1 (MRN) complex is the key sensor in DSB, and upon activation relays the information to the ATM and ATR kinases (Zhou and Paull, 2013). These kinases signal the mediators (53BP1, BRACA1) and activate effectors Chk2 (ATM

pathway) and Chk1 (ATR pathway). The effector kinases cross talk with various components downstream such as cell cycle regulators as well as transcription factors (Fig 1.2).

Table 1. Factors involved in DNA strand break repair and damage signaling in budding yeast and mammals

| | Mammals | Yeast (<i>S. cerevisiae</i>) |
|--|--|---|
| <u>DNA strand break repair</u> | | |
| NHEJ | | |
| End binding | MRE11–RAD50–NBS1(MRN) Yku70–Yku80 DNA-PKcs | Mre11–Rad50–Xrs2 (MRX) Ku70–Ku80 |
| End processing | Artemis, APLF, PNK, APTX | |
| Ligation | LigaseIV–XRCC4–XLF | Lig4–Lif1–Ner1 |
| HR | | |
| Resection | MRN, CtIP, EXO1, BLM, DNA2? | MRX, Sae2, Exo1, Sgs1, Dna2 |
| Homologous pairing and strand exchange | RPA, RAD51, RAD52, RAD54, RAD51 paralogs BRCA2–PALB2 (=FANCD1–FANCN) | Rfa, Rad51, Rad52, Rad54, Rad55–Rad57 |
| DNA synthesis | PCNA, Pol δ | PCNA, Pol δ |
| HR resolvases | MUS81–EME1, GEN1, SLX1–SLX4, XPF–ERCC1 | Mus81–Eme1, Yen1 Slx1Slx4, Rad1–Rad10 |
| Dissolution of HR intermediates | BLM–TOPOIII–RMI1–RMI2, RTEL1 | Sgs1–Top3–Rmi1, Srs2 |
| SSBR | | |
| Detection | PARP-1 | |
| End processing | APE1, XRCC1, PNK, APTX | |
| Gap filling, ligation | LigIII, Pol β | |
| <u>DNA damage signaling</u> | | |
| Sensors | | |
| | MRN RPA (+RFC-like, PCNA-like checkpoint clamp) | MRX Rfa (+RFC-like, PCNA-like checkpoint clamp) |
| Transducers | | |
| | ATM ATR–ATRIP | Tel1 Mec1–Ddc2 |
| Mediators | | |
| ATM signaling | 53BP1, MDC1, BRCA1, MCPH1 PTIP | Rad9 |
| ATR signaling | TopBP1 Claspin | Dpb11 Mrc1 |
| Effectors | | |
| | CHK1 CHK2 | Chk1 Rad53 |

Figure 1.2: Table listing the factors involved in DNA double strand break repair and damage signaling in budding yeast and mammals. Adapted from Polo and Jackson, 2011.

Hence, Telomere dysfunction marked by A persistent DNA damage signaling leads to rampant genome duplications and deletions (Batista and Artandi, 2009). These genomic instabilities lead to Telomerase activation - a ribonucleoprotein that specializes in adding new telomere sequences onto chromosome ends (Greider and Blackburn, 1987). The telomeres, due to the end replication problem, are shortened progressively after each cell division and hence have been hypothesized to act as a molecular clock associated with age related

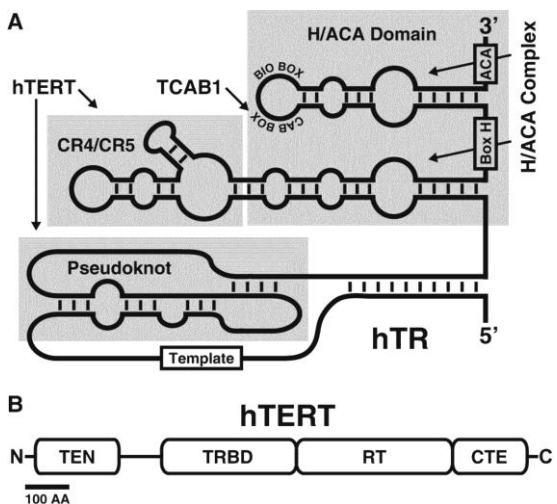


Figure 1.3: Functional domains of (A) hTERT and (B) hTERT. Adapted from Schmidt and Cech, 2015.

pathologies and also in triggering senescence. However in stem cells and germ cells, Telomerase ensures that a critical telomere length is maintained. Human Telomerase consists of hTR and hTERT in association with its accessory proteins such as dyskerin, NOP10, NHP2 and GAR1 (Schmidt and Cech, 2015) (Fig 1.3). TERT is silenced following embryogenesis as a tumor suppressive mechanism and is unregulated in ~85% of human cancers (Shay and Bacchetti, 1997). Mutations in any of the telomerase components or accessory proteins results in telomerase deficiency syndromes such as Dyskeratosis congenita, Aplastic anemia - which are characterized by genomic instability and accelerated ageing. Therefore along with telomeres, Telomerase also regulates the process of ageing (Jaskelioff et al., 2011; Wang et al., 2000). In addition, telomere dysfunction coupled with Telomerase activation drives tumor growth and progression (Ding et al., 2012). Even though Telomerase has been largely attributed to elongating Telomeres, studies have hinted on non-canonical functions of Telomerase ranging from cell proliferation, apoptosis and mitochondrial dysfunction (Martínez and Blasco, 2011) . However, the mechanistic details as well as physiological relevance remains largely elusive.

DNA Damage Response is multi-factorial, and Lamin A is the new addition in the plethora of proteins that assist DDR. MEFs in which nuclear envelope protein Lamin A was down regulated also showed a down regulation of 53BP1 and end to end chromosome fusion in de-protected telomeres (Gonzalez-Suarez et al., 2009). Interestingly further investigation revealed that lamin A deficient cells have impaired NHEJ due to reduced levels of 53BP1. In addition it was found that lamin A depletion also hampered HDR by indirect regulation of the levels of key mediators of the pathway BRACA1

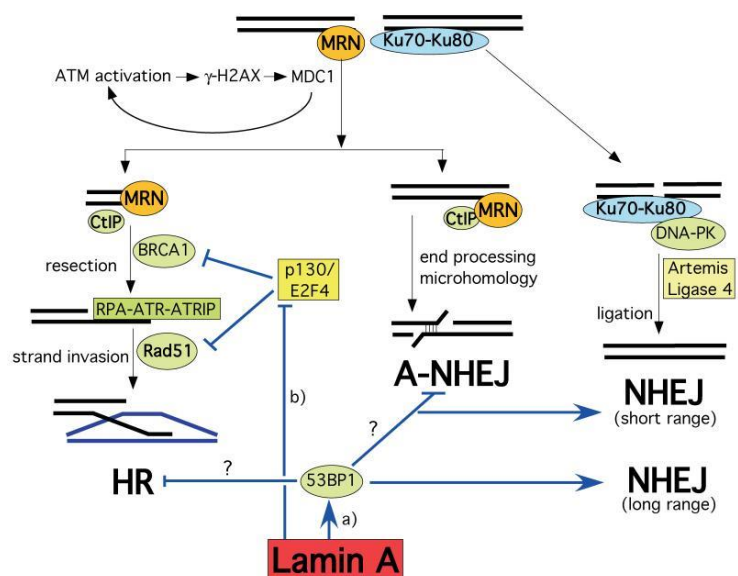


Figure 1.4: Role of Lamin A in DNA damage repair pathways. Adapted from Brachner and Foisner, 2011.

and RAD51, suggesting intricate crosstalk between lamin A and different DNA repair pathways (Redwood et al., 2011) (Fig 1.4). Lamin A is a part of the nuclear Lamina which consists of complex protein network at the nuclear periphery and is associated with chromatin (Fawcett, 1966). Lamins are type V intermediate filament proteins. Proteins belonging to this gene family are involved in forming strong networks and helps in scaffolding. Lamins assemble into a filamentous meshwork beneath the inner nuclear membrane (Goldman et al., 1986). The organization of Lamins at the nuclear periphery is also regulated by Lamin-binding proteins (Dorner et al., 2007). Lamins are classified as A- or B-type Lamins. The major isoforms of A-type Lamins are Lamin A and Lamin C. Both arise from the gene *LMNA*, by alternative splicing. B-type Lamins are B1, B2, & B3 of which the most abundant are Lamin B1 and Lamin B2, encoded by separate genes, *LMNB1* and *LMNB2*, respectively. *LMNB2* expresses the minor isoform B3 (Peter et al., 1989). Lamin A also associates with TRF2 (Wood et al., 2014). Telomeres are tethered to the nuclear envelope and Lamin A plays a pivotal role in maintaining its organization in the interphase nucleus (Gonzalez-Suarez et al., 2009).

Spectrum of diseases that share strikingly similar traits with the telomere syndromes are those caused by mutations in Lamin A. Termed as Laminopathies, these diseases are characterized by nuclear morphological abnormalities, disorganization of heterochromatin, telomere attrition, defects in DNA damage response and accelerated ageing (Kudlow et al., 2007). In addition, Lamin A/C deficient cells are sensitive to agents that cause inter-strand crosslinks and increases chromosomal aberrations (Singh et al., 2013). Also recent evidence of extra Telomeric roles of telomerase dictate that it has a protective role against DNA damaging agents and increases tolerance to chromosomal instability (Fleisig et al., 2016). Telomerase overexpressing cells showed increased levels of DNA Damage Repair proteins - KU70-80 (Cao et al., 2014).

We therefore aim to investigate the roles of Lamin A and Telomerase in the DNA damage response pathway. The proliferative defects induced in cells upon Lamin A mutants are rescued by the induction of Telomerase (Kudlow et al., 2008). However, fibroblasts derived from progeria patients undergo senescence despite having active

levels of Telomerase (Wallis et al., 2004). Telomerase expression shows an inhibitory effect on progerin production (Cao et al., 2011). However, the co-regulatory role of Lamin A and Telomerase in the context of DNA Damage Response remains unclear. Understanding the link between the two is of importance since it may provide new insights in diseases such as laminopathies and cancer. Hence this project aims to investigate and dissect the potential crosstalk between Lamin A and Telomerase in DNA Damage Response.

MATERIALS & METHODS

Materials

| Reagent | Components |
|-----------------------------------|--|
| 10 X SDS RUNNING BUFFER (1 litre) | <ul style="list-style-type: none">• Tris 30.3 g• Glycine 144.1 g• SDS 10 g• Dissolve the components in 800 ml Distilled water, and then make up the volume to 1000ml |
| 10 X TRANSFER BUFFER (1 litre) | <ul style="list-style-type: none">• Tris 30.3 g• Glycine 144.1 g• Dissolve the components in 800 ml Distilled water, and then make up the volume to 1000 ml. |
| 10 X TRANSFER BUFFER (1 litre) | <ul style="list-style-type: none">• 100 ml 10 X Transfer Buffer• 100 ml Methanol• 800 ml Distilled water |
| 10 X TBS (1 litre) | <ul style="list-style-type: none">• Tris 60.5 g• Sodium Chloride 87.6 g• Dissolve the components in 800 ml Distilled Water; adjust the pH to 7.5 with conc. HCl and make up the volume to 1000 ml. |
| 1 X TBST (1 litre) | <ul style="list-style-type: none">• 10 X TBS 100 ml• Distilled Water 900 ml• Tween-20 1 ml |
| 4 X LAEMMLI'S BUFFER (SDS GEL | <ul style="list-style-type: none">• 8% SDS• 4% β-Mercaptoethanol 10• 40% Glycerol• 0.08% Bromophenol Blue• 0.05M EDTA |

| | |
|---|--|
| LOADING BUFFER) | <ul style="list-style-type: none"> • 0.2M Tris – Cl (pH 6.8) |
| 7% RESOLVING GEL | <ul style="list-style-type: none"> • MilliQ Water 3.70 ml • 30% Acrylamide 1.75 ml • 1.5M Tris (pH 8.8) 1.95 ml • 10% SDS 75 µl • 10% Ammonium Persulphate 75 µl • TEMED 3 µl |
| 5% STACKING GEL | <ul style="list-style-type: none"> • MilliQ Water 2.1ml • 30% Acrylamide 495 µl • 1M Tris (pH 6.8) 375 µl • 10% SDS 30µl • 10% Ammonium Persulphate • 3 µl TEMED |
| 10X PBS (1 litre) | <ul style="list-style-type: none"> • Na₂HPO₄·7H₂O 12.91 g • NaH₂PO₄·H₂O 2.35 g • NaCl 87.66 g |
| BLOCKING BUFFER FOR WESTERN BLOT ANALYSIS | <ul style="list-style-type: none"> • 5% non-fat dried skimmed Milk in 1X TBST |
| RADIO IMMUNOPRECIPITATION ASSAY (RIPA) BUFFER | <ul style="list-style-type: none"> • Tris (pH 7.4) 50mM • NaCl 150mM • EDTA 1mM • Glycerol 8% • NP-40 1% • SDS 0.1% • Sodium Azide 0.01% • Sodium Deoxycholate 0.5% • For preparing Modified RIPA Buffer, add Roche® Protease Inhibitory Cocktail (EDTA free, Cat. No. 04 693 132 001) at the final concentration of 1X |
| CSK BUFFER | <ul style="list-style-type: none"> • 0.1M NaCl • 0.3M Sucrose • 3mM MgCl₂ |

| | |
|--|---|
| | <ul style="list-style-type: none"> • 10mM PIPES • Adjust pH to 7.4 and add 250µl Triton X-100 for every 50ml buffer |
|--|---|

Antibodies

| ANTIBODY | DILUTION | COMPANY | CATALOG NO. |
|---------------------------------|----------------------------|------------|-------------|
| Rabbit α Lamin A | 1:1000 (WB) 1:500 (IFA) | Abcam | ab26300 |
| Rabbit α GAPDH | 1:5000 (WB) | Sigma | G9545 |
| Mouse α Lamin B2 | 1:400 (WB/IFA) | Abcam | ab8983 |
| Rabbit α Lamin B1 | 1:1000 (WB) | Abcam | ab16048 |
| Mouse α TRF2 | 1:250 (WB/IFA) | Abcam | ab13579 |
| Goat α hTERT | 1:500 (WB) | Santa Cruz | sc7215 |
| Rabbit α 53BP1 | 1:200 (WB/IFA) | Abcam | ab21083 |
| Rat α Tubulin | 1:6000 | Abcam | ab6161 |
| Donkey α Rabbit HRP (secondary) | 1:10000 (WB) | GE | NA9340V |
| Sheep α Mouse HRP (secondary) | 1:10000 (WB) | GE | NA1390V |
| Goat anti Rat HRP | 1:10000 | Abcam | ab97057 |

| | | | |
|--|--------------|--------------------------|-------------|
| (secondary) | (WB) | | |
| Donkey anti Goat HRP (secondary) | 1:10000 (WB) | Jackson Immuno Reasearch | 705-035-003 |
| Goat α Rabbit Alexa 488 (secondary) | 1:1000 (IFA) | Molecular probes | A11034 |
| Goat α Mouse Alexa 568 (secondary) | 1:1000 (IFA) | Molecular probes | A11004 |

Methods

Cell culture

HT1080 (human fibrosarcoma) and U2OS (human osteosarcoma) cells were cultured in DMEM (Invitrogen, 11995) in 10% heat inactivated Fetal Bovine Serum (FBS, Invitrogen, 6140-079 Carlsbad, USA) and supplemented with Penicillin (100 units) and Streptomycin (100 μ g/ml, Invitrogen, 15070-063). Cells were grown at 37°C and 5% CO₂. HT1080 cells with the Telomerase construct (ST-HT1080) were grown in DMEM in presence of 10% heat inactivated FBS and supplemented with Penicillin (100 units) and Streptomycin (100 μ g/ml) and additionally with Hygromycin (250 μ g/ml, Sigma, H3274) and G418 (1 mg/ml, Roche, 04 727 878 001). ST cells are derived from HT1080 with stable overexpression of hTERT and hTR. The cell line was a kind gift from Dr. Shantanu Choudhury, IGIB, Delhi.

hTERT overexpression

Transfection Mix (500 μ l) was prepared containing required concentration of hTERT (2 μ g), Invitrogen PLUS Reagent, Invitrogen Lipofectamine-LTX Reagent (Invitrogen, 15338100) and GIBCO OPTI-MEM (reduced nutrient medium, 31985-070). The

mixture was kept undisturbed for 30 minutes. Nutrient medium was then removed from cells seeded overnight in 6-well culture plates (0.4 million cells/well) and 1.5 ml of serum free media (DMEM) was added to each well. The Transfection Mix was then added to each well. After incubation of 5-6 hours, the serum free media with Transfection Mix was removed from the wells and 2 ml of fresh nutrient medium (DMEM) was added to each well. The cells were incubated for 48 hours. hTERT pcDNA3.1 vector contains full length hTERT cDNA in pcDNA3.1 vector backbone and is a kind gift from Dr. Shantanu Choudhury, IGIB, Delhi.

shRNA mediated transient knockdown

Transfection Mix (500 µl) was prepared containing required concentration of shRNA (6 µg), Invitrogen PLUS Reagent, Invitrogen Lipofectamine-LTX Reagent (Invitrogen, 15338100) and GIBCO OPTI-MEM (reduced nutrient medium, 31985-070). The mixture was kept undisturbed for 30 minutes. Nutrient medium was then removed from cells seeded overnight in 6-well culture plates (0.4 million cells/well) and 1.5 ml of serum free media (DMEM) was added to each well. The Transfection Mix was then added to each well. After incubation of 5-6 hours, the serum free media with Transfection Mix was removed from the wells and 2 ml of fresh nutrient medium (DMEM) was added to each well. The cells were incubated for 48 hours followed by seeding them in 100mm dish under puromycin selection (400 ng/ml, Invitrogen, A1113802) for HT1080 cells and U2OS cells for colony picking.

shRNA sequence used:

LMNA shRNA_5 (Sigma TRC1.5 vector backbone, pLKO.1-puro)

5'CCGGCCCACCAAAGTTCACCCTGAACTCGAGTTCAGGGTGAAC TTTGGTGGGTT
TTTG 3'

Colony Isolation

Colonies of cells were isolated using Sigma Aldrich sterile cloning disks (Sigma, Z374431-100EA). The colonies that were to be picked were marked and media was

removed from the plate. The cells were then rinsed in sterile DPBS (Invitrogen, 14190-144). The cloning disc immersed in trypsin (Invitrogen, 25300-054) was placed on marked conies and incubated for 2-3 minutes. The discs were then removed and transferred to a 24 well plate with 500 μ l medium.

Preparation of whole cell lysates

Whole cell lysates were prepared in Radio Immuno Precipitation Assay (RIPA) Buffer containing Roche Protease Inhibitor Cocktail (PIC) at concentration of 1X. The cells were scraped in ice-cold buffer, incubated on ice for 15 mins with slow shaking and centrifuged at 14000 rpm/4°C/20 mins. The lysates were stored at -20°C.

Protein estimation of whole cell lysate

Protein estimation of the whole cell lysate was carried out by Bicinchoninic Acid (BCA) method using the Pierce BCA Protein Assay Kit (Pierce, 23225). Protein standards were prepared using Bovine Serum Albumin (BSA) from a concentration of 0.0 – 2.0 mg/ml. Samples were estimated at 1:1 dilution and RIPA Buffer with 1X Protease Inhibitor Cocktail (PIC) was used as 'Blank'.

Western Blot analysis

The protein lysate samples were resolved on a 7% or 15% Acrylamide Resolving Gel and 5% Stacking Gel at 90-100 Volts. The molecular weight markers used were Invitrogen See-Blue (198-3 kDa, Cat No. 100006636) and Bio-Rad Precision Plus Protein Standards All Blue (250-10 kDa, Cat No. 161-0373). The proteins were then transferred onto methanol-activated PVDF membrane at 90 Volts for 200 minutes. Blocking of the blot was carried out in 5% skimmed milk in 1X TBST for 1 hour at room temperature followed by three 1X TBST washes of 10 minutes each. The primary antibody was added onto the blot and incubated at room temperature for 3 hours with

slow shaking (or at 4°C overnight). This was followed by three 1X TBST washes of 10 minutes each. The secondary antibody (conjugated with Horse Radish Peroxidase) was added onto the blot and incubated at room temperature for 1 hour with slow shaking. This was followed by three 1 X TBST washes of 10 minutes each. The blot was then developed on the LAS4000 image reader using Chemiluminescent Substrate Kits (GE Healthcare ECL Prime Western Blotting Substrate, 89168-782).

Immunofluorescence assay

Cells were grown on coverslips and washed with 1X PBS and treated with cold CSK Buffer on ice for 4 mins. Cells were fixed using freshly prepared 4% paraformaldehyde solution for 12 mins, followed by two washes of 5 mins using 1X PBS. Permeabilisation of the cells was carried out using 0.5% Triton X-100 in 1X PBS for 10 mins. The cells were then blocked in 1% BSA for 30 mins at room temperature, followed by three 1 X PBS washes of 5 minutes each. The cells were then incubated with the primary antibody (in 0.5% BSA) for 90 minutes at room temperature and followed by three 1 X PBS washes of 5 minutes each. The secondary antibody (conjugated with Alexa Fluor 488 green or Alexa Fluor 568 red) was added onto the cells and incubated at room temperature for 60 minutes, followed by three 1X PBST washes of 5 minutes each. The cells were counterstained in DAPI solution (4'-6-diamidino-2-phenylindole) and after a brief 1X PBS wash, were mounted on glass slides in Invitrogen SlowFade Gold Antifade Reagent (Invitrogen, S36937). The coverslips were sealed using nail polish. Confocal images were acquired on a Zeiss LSM 710 confocal microscope (Carl Zeiss, Thornwood, NJ, USA) with a 63X Plan-Apochromat 1.4 NA oil immersion objective using charge-coupled device camera (AxioCam MRm Rev.3, Zeiss), ZEN software and scan zoom of 2.0-2.5. Z-stacked images were acquired at 512 X 512 pixels per frame using 8-bit pixel depth for each channel at a voxel size of 0.105 µm X 0.105 µm X 0.34 µm and line averaging set to 2 collected sequentially in a three channel mode. Imaging of DAPI stained metaphases was performed on the ZEISS AXIOVERT microscope with a 63X Plan-Apochromat 1.4 NA oil immersion objective.

Preparation of metaphase spreads

Control HT, ST and U2OS cells were grown to a confluency of ~60%. 10 µl/ml of Invitrogen Colcemid Solution (Roche, 10 295 892 001) was added to arrest the cells at metaphase. The cells were incubated at 37°C under 5% CO₂ for 80 minutes. The medium was removed and cells harvested by trypsinization. Cells were centrifuged at 1000 rpm, 10°C for 5 minutes; the supernatant was discarded and the pellet was resuspended in 4 ml of 0.075 M Potassium Chloride (pre-warmed to 37°C). This suspension was incubated in a water-bath at 37°C for 30 minutes. After the incubation, few drops of the fixative (freshly prepared 3:1 solution of Methanol: Acetic Acid) was added to terminate the reaction. This suspension was centrifuged at 1200 rpm and 4°C for 10 minutes and washed thrice in fixative. ~10 µl of this suspension was dropped onto glass slides from a height. The metaphase spreads were allowed to dry. The metaphases were stained with 0.05 µg/ml DAPI solution for 2 mins and mounted in Invitrogen SlowFade Gold Antifade Reagent.

RNA extraction and RT PCR

Primers used for the RT PCR reaction:

| Gene | Primer sequences |
|-------|---|
| LMNA | (F) 5' CCGCAAGACCCTTGACTCA 3' (R) 5' TGGTATTGCGCGCTTTCAG 3' |
| LMNB1 | (F) 5' CGACCAGCTGCTCCTCAACT 3' (R) 5' CTTGATCTGGGCGCCATTA 3' |
| LMNB2 | (F) 5' AGTTCACGCCCAAGTACATC 3' (R) 5' CTTCACAGTCCTCATGGCC 3' |
| hTERT | (F) 5' CGGAAGAGTGTCTGGAGCAA 3' (R) 5' TCGTAGTTGAGCACGCTGAACAG 3' |
| GAPDH | (F) 5' CGAGATCCCTCCAAAATCAAG 3' (R) 5' GCAGAGATGATGACCCTTTTG 3' |

RNA Extraction

- (a) Homogenization of the sample: Post 48 h after the transfection. The media was removed from 6 well plates and was washed using 1X PBS. To the washed wells 500µl of TRIZOL reagent (Invitrogen, 15596-026) was added to homogenize the cells. The plates were incubated at RT for 5 minutes followed by collecting the samples in 1.5ml eppendorfs for phase separation.
- (b) Phase separation: To the sample, 100 µl Chloroform (per 500µl of TRIZOL) was added. The mixture was inverted 40 times without vortexing and was incubated at RT for 10 mins. The sample was centrifuged for 15 minutes at 4°C and 12000g. The aqueous phase was collected and 500 µl of Isopropanol was added. The mixture was incubated at RT for 10 mins followed by centrifugation 15 minutes at 4°C and 12000g.

The pellet was dislodged using 75% ethanol in nuclease free water. The sample was centrifuged for 15 minutes at 4°C and was kept for drying at RT. To the dried pellet 10-15 µl RNAase free water was added and samples were incubated at 37 °C for 10 minutes.

cDNA preparation

cDNA was prepared with ImProm-II Reverse Transcriptase System (Promega, A3800). Scheme followed:

(a) RNA mix (5µl reaction)

| Components | Stock concentration | Volume added/Final concentration |
|--------------|---------------------|----------------------------------|
| Purified RNA | | x µl (1 µg) |
| Oligo dT | 50 µg | 1 µl (2.5 µg) |
| NFW | | 5 - (1+x) µl |

After the addition of Oligo dT, the samples are incubated at 70°C for 5 minutes followed by quick chill of 2 mins on ice.

(b) Reverse Transcriptase mix (15 µl reaction)

| Components | Stock concentration | Volume added/Final concentration |
|---------------------------|---------------------|----------------------------------|
| ImProm-II reaction Buffer | 5x | 4 µl (1X) |
| Mgcl ₂ | 25 mM | 2.4 µl (3 mM) |
| dNTP | 10 mM | 1 µl (0.5 mM) |
| RNAsin | 20 U | 0.5 U |
| Reverse Transcriptase | 20 U | 1 U |

PCR Reaction scheme:

1. 25°C for 15 minutes
2. 42°C for 60 minutes
3. 75°C for 5 minutes
4. 4°C

RT PCR

(a) Kapa Sybr Mix (4 µl reaction)

| Components | Stock concentration | Volume added/Final concentration |
|--|---------------------|----------------------------------|
| Kapa Sybr Green KAPA Biosystems (KM4100) | 100x | 2.5 µl |
| Forward+Reverse Primer cocktail | 10 µM | 0.2 µl (0.4 µM) |
| Nuclear free water | | 1.3 µl |

In each well of a 96 well PCR plate, 4 µl of Sybr mix and 1 µl of 1:3 diluted cDNA was added along with appropriate cDNA and Primer controls.

RT PCR (Biorad CFX96) reaction scheme:

- (a) 95°C for 5 minutes
- (b) 95°C for 20 seconds
- (c) 60°C for 1 minute

Transcript levels were determined after normalizing with GAPDH and further normalizing with respect to Vector control or HT1080 levels. Relative levels were obtained using $2^{-(\Delta\Delta ct)}$ method.

DNA Damage using Cisplatin

0.8 million cells were seeded per well over night for treatment with cisplatin (Sigma, P4394). The following concentration range of cisplatin was used: 0, 10, 25, 50 and 100 μ M cisplatin (prepared from 16.6 mM stock) and was added to cells for 3 hours, after which the cells were processed for immunofluorescence assays or western blotting.

53BP1 Foci count, Distance measurement from the periphery and Statistical analysis

TRF2 and 53BP1 foci number and intensity measurement were performed using ImageJ. 53BP1 foci counting and distance measurement in Control and shLMNA cells was performed using Huygens Software (Scientific Volume Imaging). Statistical analysis was performed with Mann Whitney Wilcoxon sum rank test and ANOVA using Graph Pad Prism 5.0 software, p-value < 0.05 was considered to be statistically significant. Graphs were plotted using Graph Pad Prism 5.0.

RESULTS

The aim of this project is to address the molecular interplay between Lamin A and Telomerase in regulating DNA damage response. More specifically we asked whether Lamin A participates in the protective role that Telomerase confers in alleviating DNA damage. We examined the effect of Telomerase on the levels of Lamins. Further we downregulated Lamin A in HT1080 (Telomerase positive), U2OS (Telomerase negative) cells and examined its effects on 53BP1 - an important factor in the Non-Homologous End-Joining pathway (NHEJ) that mediates double strand break repair.

1. Levels of Lamins are relatively lower in hTERT overexpressing cells

In order to examine the roles of Lamin A and hTERT in the context of DNA damage, we first determined the levels of Lamins and hTERT in cell lines that express differential levels of hTERT (i) HT1080 - a fibrosarcoma cell line (HT, Telomerase, positive) (ii) ST-HT1080 (HT1080 stably transfected to overexpress hTERT or referred to as ST) and (iii) U2OS – an osteosarcoma cell line, Telomerase negative. Whole cell lysates were prepared from proliferating HT, ST and U2OS cells and levels of Lamins, hTERT and 53BP1 was determined.

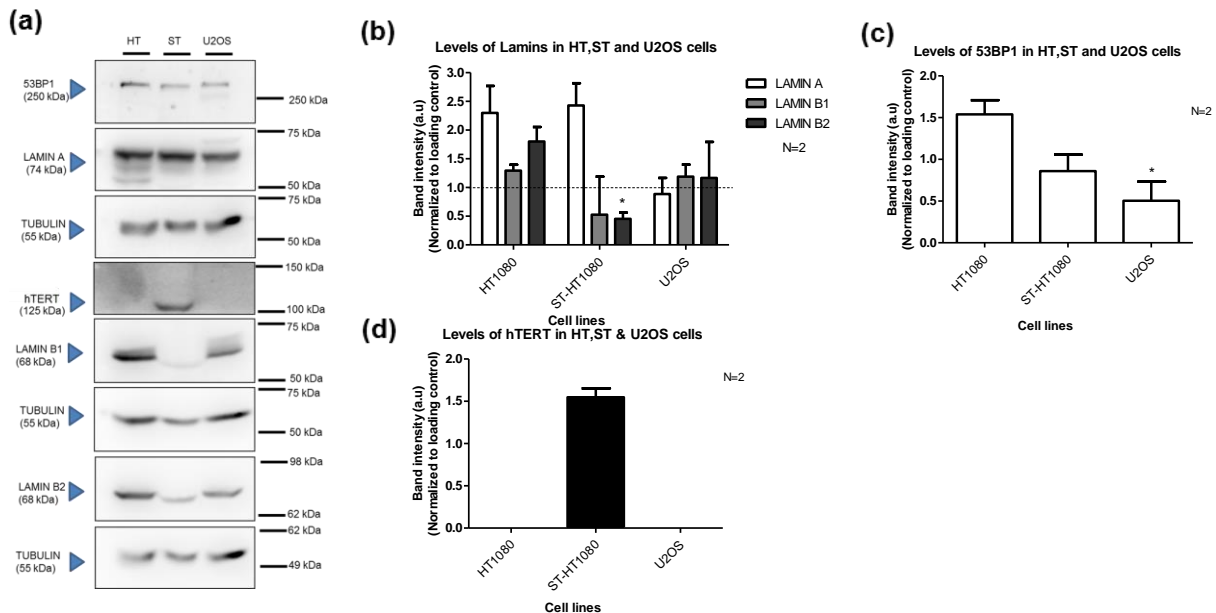


Figure 2.1: Expression levels of Lamins, hTERT and 53BP1 in HT1080, ST-HT1080 and U2OS cells (a) Western blots showing levels of Lamin A, B1, B2, hTERT and 53BP1 (b) Levels of Lamins in HT, ST and U2OS cells (c) & (d) Levels of 53BP1 and hTERT in HT, ST and U2OS cells. Levels were quantified with respect to the loading control Tubulin (N = biological replicates, *: p<0.05)

Quantification of protein levels from western blots (Fig 2.1a) show that as compared to HT1080, B-type lamin levels are relatively lower than Lamin A in ST-HT1080 cells (Fig 2.1b). In U2OS cells, Lamin B1 levels are comparable to that of HT1080 while Lamin B2 levels are intermediate to HT and ST cells. Lamin A is robustly expressed in both HT and ST cells while in U2OS cells the levels are lower as compared to HT and ST cells (Fig 2.1b). Out of the three cell lines tested, 53BP1 levels were relatively higher in HT1080 cells and lowest in U2OS cells. Notably, 53BP1 levels were significantly lower in cells overexpressing Telomerase corroborating role of Telomerase in DNA damage (Fig 2.1c). Both HT1080 and U2OS did not express detectable levels of hTERT, while ST cells show significant hTERT expression (Fig 2.1d). These results suggest an inverse correlation between levels of Telomerase and Lamins.

2. Transcript levels of B-type Lamins are relatively lower in ST-HT1080 cells.

These experiments revealed that B-type Lamins show lowered levels in ST cells compared to HT1080 cells. We therefore examined the relative transcript levels of Lamin genes (*LMNA*, *LMNB1* and *LMNB2*) to examine whether lowered protein levels could be attributed to a downregulation of these genes at the transcript level. We performed RT-PCR to determine the relative expression levels of transcripts in HT1080, ST-HT1080 and U2OS cells.

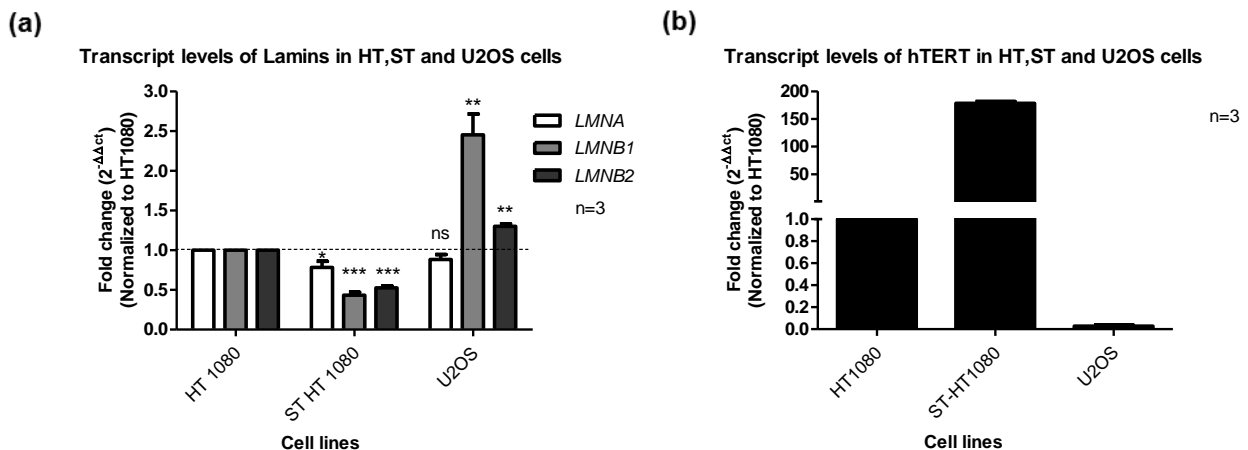


Figure 2.2: Transcript levels of Lamins and hTERT in HT1080, ST-HT1080 and U2OS cells
(a) Transcript levels of Lamin A, B1 and B2. Transcript levels are first normalized to internal control (GAPDH) and then re-normalized to Lamin levels in HT1080 cells. **(b) Transcript levels of hTERT in HT1080, ST-HT1080 and U2OS,** (n = Technical replicates. ns: $p > 0.05$, *: $p < 0.05$, **: $p < 0.01$, ***: $p < 0.001$)

At the transcript level as well, levels of B-type Lamins are significantly lower in ST-HT1080 cells as compared to HT1080 cells (Fig 2.2a). In U2OS cells however, as compared to HT1080 cells, transcript levels of B-type Lamins are significantly higher than Lamin A (Fig 2.2a). In contrast, hTERT was hardly expressed in U2OS cells while ST cells show massively elevated transcript levels of hTERT (~200 fold) relative to HT1080 cells (Fig 2.2b). This is consistent with the telomerase negative status of U2OS cells (Henson et al., 2005).

3. Levels of Lamins and hTERT across cancer cell lines.

We next asked if the levels of Telomerase correlate with Lamin levels across cancer cell types. Since, endogenous levels of hTERT are relatively lower in majority of cancer cells and protein levels by western blot would be difficult to capture (Xi and Cech, 2014). We tested for hTERT transcript levels across various cancer cell lines by RT-PCR analysis (Fig 2.3).

Transcript levels of Lamins and hTERT across cell lines

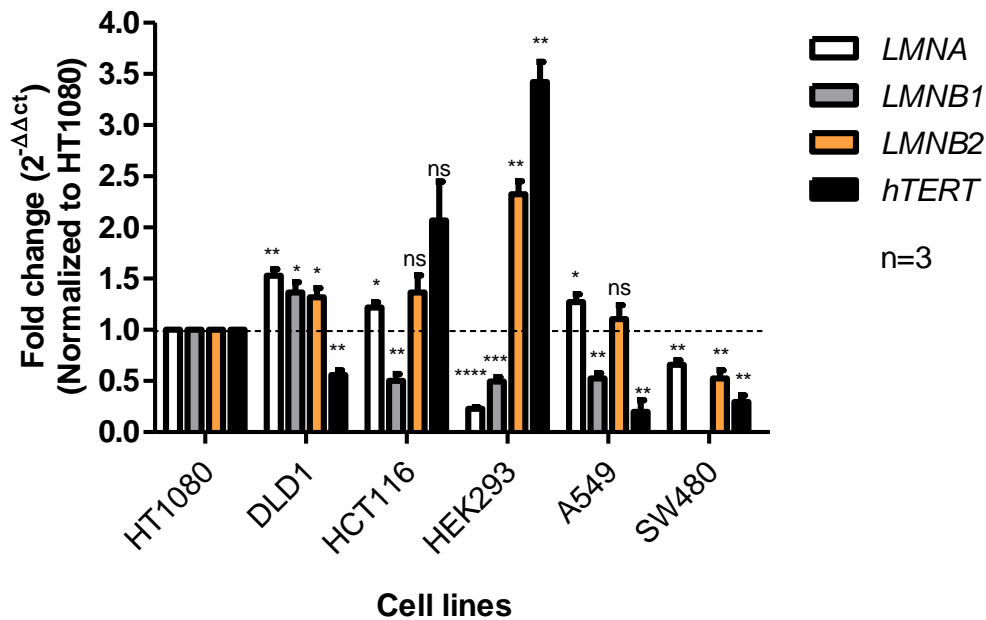


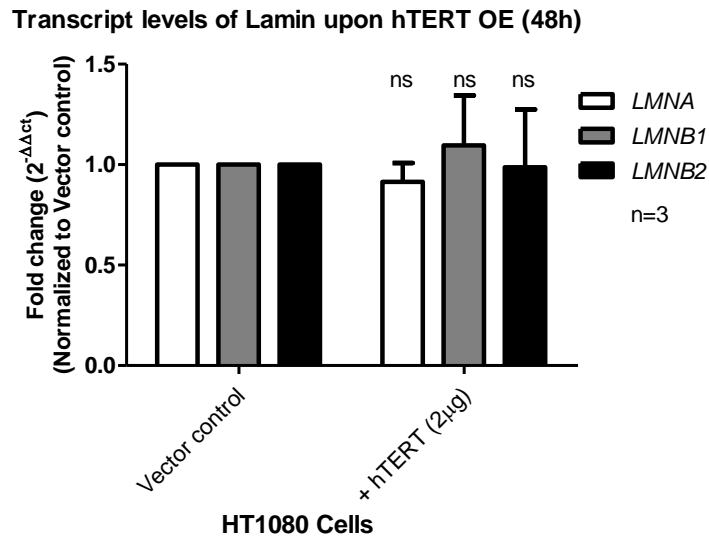
Figure 2.3: Transcript levels of Lamins and hTERT across cancer cell lines. Relative Transcript levels of Lamin A, B1, B2 and hTERT in DLD1, HCT116, HEK293, A549 and SW480 with respect to HT1080. Transcript levels were first normalized to internal control (GAPDH) and then re-normalized to Lamin levels in HT1080 cells, (n = Technical replicates. ns: p>0.05, *: p<0.05, **: p<0.01, ***: p<0.001, ****: p<0.0001)

RNA extracted from DLD1 and SW480 (Colorectal adenocarcinoma), HCT116 (Colorectal carcinoma), A549 (Lung carcinoma) and HEK293 cells were used to determine transcript levels of Lamins and hTERT and to determine if a correlation exists between the transcript levels of Lamins and hTERT (Fig 2.3). DLD1, SW480 and A549 cells show relatively lower levels of hTERT as compared to HT1080 cells, while levels of hTERT was significantly elevated in HCT116 (~2 fold) and HEK293 cells (~3.5 fold) as compared to HT1080 cells. SW480 show relatively lower levels of Lamin B2 (~0.4 fold), while in HEK293 cells, Lamin B2 is significantly overexpressed (~2.5 fold). Levels of B2 are largely comparable in all the other cell lines. Lamin B1 transcript levels were significantly lower in HCT116 and HEK293 cells, in which Telomerase levels are higher than HT1080 and all the other cell lines that were tested (Fig 2.3). Interestingly, Lamin A was significantly downregulated in HEK293 cells compared to HT1080 cells. However, in A549 cells, Lamin B1 levels are relatively lower despite lower levels of telomerase with respect to HT1080 (Fig 2.3). Taken together this data reveals that Lamin B1 transcript levels are significantly downregulated than Lamin A, B2 and shows a negative correlation compared to transcript levels of hTERT in HCT116 and HEK293 cells (Fig 2.3)

4. Effect of hTERT overexpression on transcript levels of Lamins in HT1080 and U2OS cells

Our studies reveal that the negative correlation of Lamins and hTERT is cell type specific (Fig 2.3). We next, overexpressed hTERT in HT1080 cells and U2OS cells respectively, to examine if a transient overexpression of hTERT modulates levels of Lamins as seen in ST-HT1080 cells (Fig 2.2a).

(a)



(b)

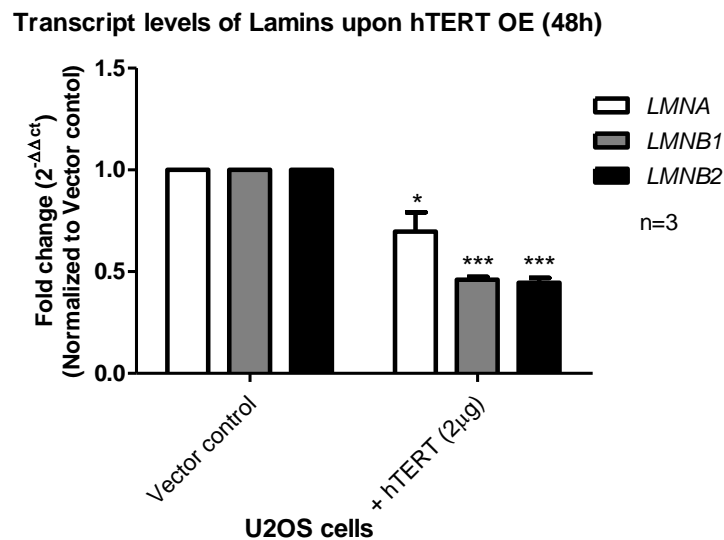


Figure 2.4: Transcript levels of Lamins upon hTERT overexpression in HT1080 and U2OS cells (a) Transcript levels of Lamin A, B1 and B2 upon hTERT transfection in HT1080 cells after 48 hours (b) Transcript levels of Lamin A, B1 and B2 upon hTERT transfection in U2OS cells after 48 hours. Transcript levels were first normalized to internal control (GAPDH) and re-normalized to Lamin levels in vector control, (n=Technical replicates. ns: $p > 0.05$, *: $p < 0.05$, **: $p < 0.01$, *: $p < 0.001$, ****: $p < 0.0001$)**

2 μ g of hTERT vector (pcDNA3.1) was transfected into proliferating HT1080 and U2OS cells. RT-PCR analysis after 48 hours did not show any effect on Lamin levels in HT1080 cells (Fig 2.4a). However, in Telomerase negative U2OS cells, overexpression of hTERT significantly lowered the levels of Lamin A (~0.7 fold), B1 and B2 (~0.4 fold) compared to the vector control in 48 hours (Fig 2.4b).

5. hTERT Overexpression does not interfere with the ALT Mechanism

Cancer cells express Telomerase to overcome replicative senescence and to proliferate indefinitely (Kim et al., 1994). However, not all cancers are Telomerase positive and these cancers maintain their Telomere length by means of Homologous recombination, Break induced replication without involving Telomerase (Bryan et al., 1997). These Telomerase independent mechanisms are commonly referred to as Alternative Lengthening of Telomeres (ALT). ALT mechanism can be probed by examining levels of ALT associated Promyelocytic Leukemia (PML) bodies (APB) (Fasching et al., 2005). Since APB's are active sites housing DNA repair proteins (Draskovic et al., 2009; Wu et al., 2000), Telomere foci are typically associated with PML bodies in an ALT positive cell line. We examined if the observed down regulation of Lamins upon Telomerase overexpression is independent of Telomere elongation, by association of Telomere foci with PML bodies (Fig 2.5).

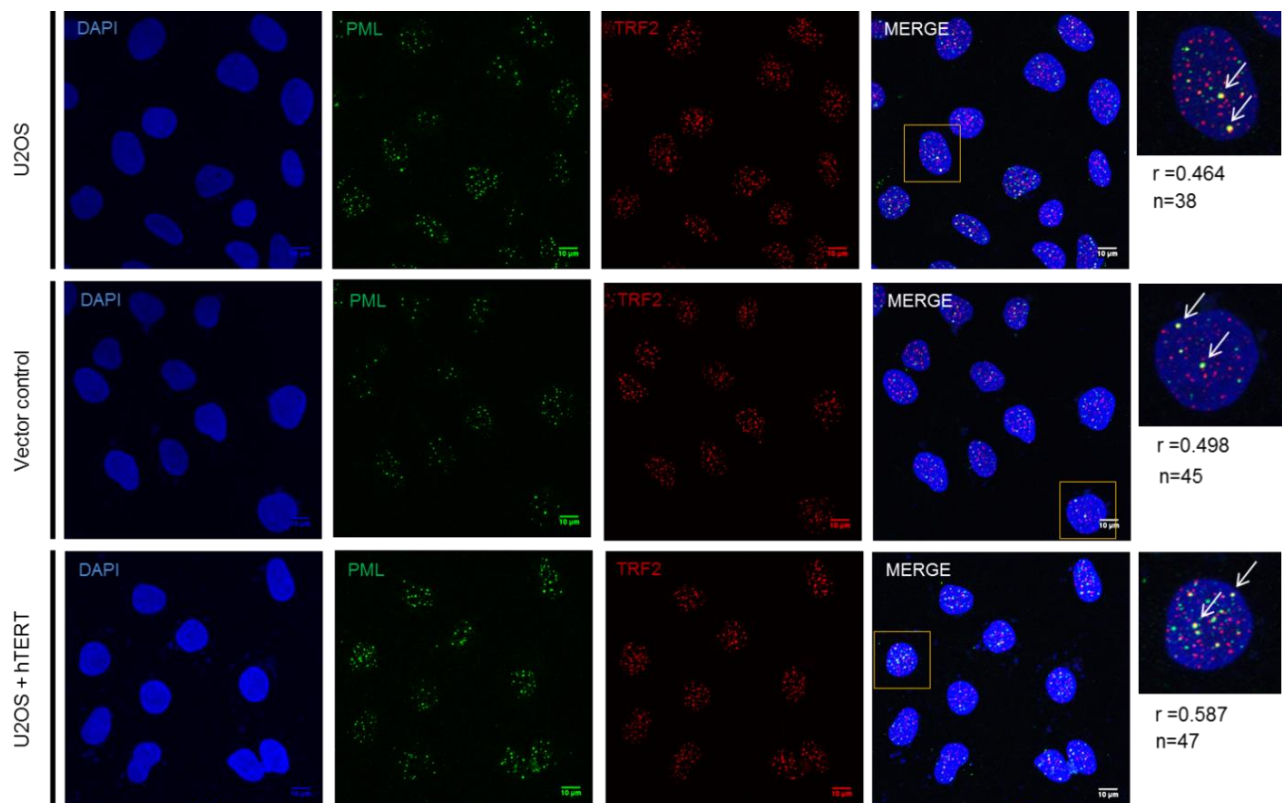


Figure 2.5: ALT associated PML bodies in control U2OS, vector control and hTERT transfected U2OS cells. Zoomed image of a single nucleus that depicts the extent of co-localization between TRF2 and PML (r: Pearson's Coefficient of Correlation calculated and n is the number of nuclei analyzed), scale bar = 10µm.

In order to probe for APB's, U2OS cells were transfected with hTERT and vector control and immunostained stained for TRF2 (to probe for Telomeres) and PML bodies. Confocal imaging and analysis revealed a positive correlation (Pearson's coefficient $r=0.49$ and 0.58 , Fig 2.5), indicating marginal co-localization between TRF2 and PML foci. The extent of co-localization is comparable with the vector control indicating functional ALT mechanism for Telomere elongation. Thus, downregulation of B-type Lamins at the transcript level (Fig 2.4) can be attributed to non-canonical functions of the Telomerase enzyme.

6. Telomere status in Telomerase proficient cell lines (HT1080 and ST-HT1080) and Telomerase deficient cells (U2OS).

Since the cell lines differ significantly in terms of their Telomerase levels (Fig 2.1d, Fig 2.2b), we examined the status of Telomeres in these cell lines. We probed for number of Telomere foci by immunostaining cells for TRF2 and counting the number of TRF2 foci per nuclei in all the three cell lines (Fig 2.6).

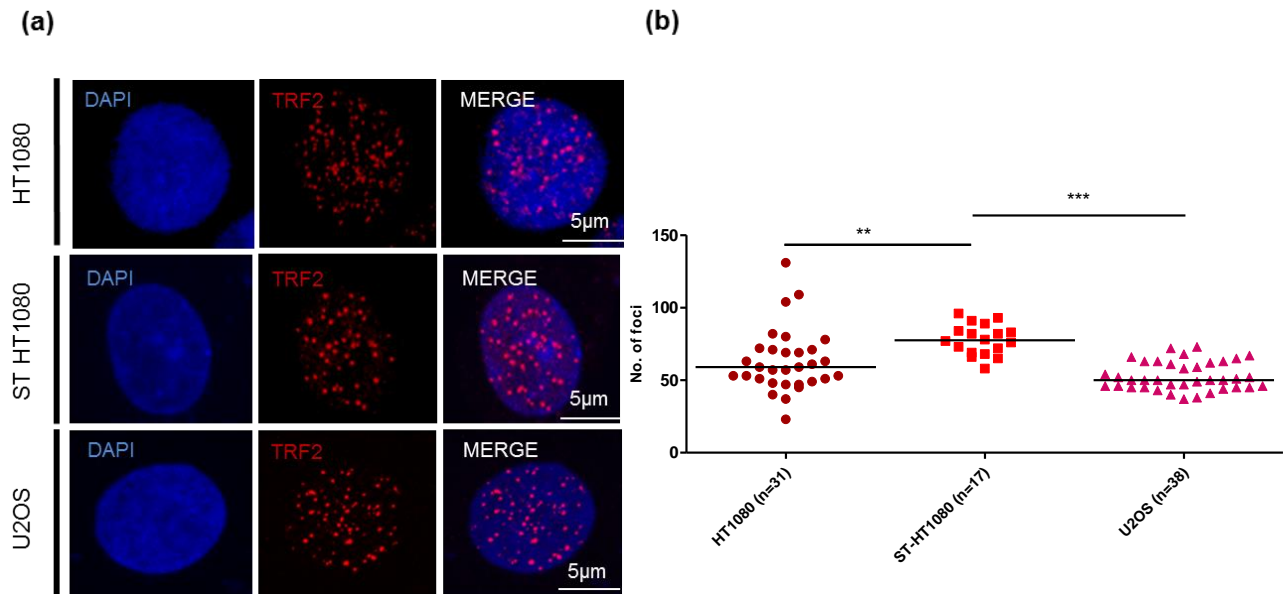


Figure 2.6: TRF2 staining and quantification in HT1080, ST-HT1080 and U2OS cells (a) Representative zoomed in image of a single nuclei of HT1080, ST-HT1080 and U2OS cells bearing the TRF2 foci (b) Quantification of TRF2 foci per nuclei in all the cell lines (Mean foci number : HT1080 - 62, ST-HT1080 - 82, U2OS - 52), n = Number of nuclei, *: $p < 0.05$, **: $p < 0.01$, *: $p < 0.001$, ****: $p < 0.0001$)**

TRF2 foci quantification revealed ST-HT1080 cells have relatively higher numbers of TRF2 foci/nuclei (82) compared to HT1080 (62) and U2OS (52) cells (Fig 2.6b). This increase in number of TRF2 foci suggests an impact of hTERT overexpression on the overall ploidy of ST-HT1080 cells.

7. Stable overexpression of hTERT renders HT1080 cells (ST-HT1080) Hypo-tetraploid

Compared to both HT1080 and U2OS cells, TRF2 foci per nuclei in ST-HT1080 are higher, suggesting an effect of Telomerase on the overall ploidy of cells. We therefore determined the ploidy of the three cell lines by counting chromosome numbers from independent metaphase spreads (Fig 2.7a-c).

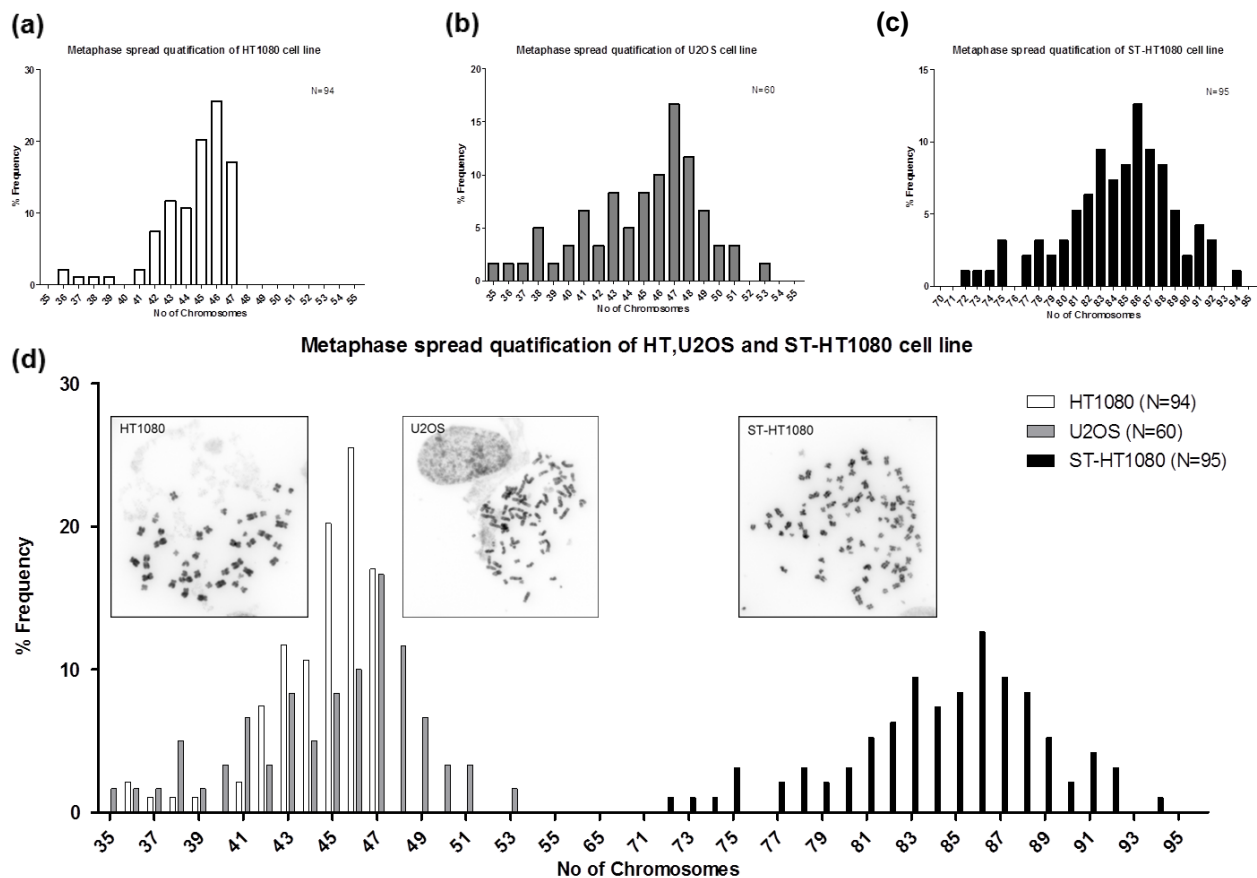


Figure 2.7: Quantification of chromosome numbers from metaphase spread derived from (a) HT1080 (Modal number = 46) (b) U2OS (Modal number = 47) and (c) ST-HT1080 cells (Modal number = 86) (d) Combined graph for (a), (b) and (c). Insets in (d) depicts representative metaphase spreads from each cell line (N= Number of Metaphase spreads analyzed).

Metaphase spread quantification reveals that HT1080 is pseudodiploid with modal number of ~46 chromosomes (Fig 2.7a). U2OS cells (~17%) have 47 chromosomes, while there are minor populations (<5%) with >50 chromosomes (Fig 2.7b). In contrast to HT1080 and U2OS cells, ST cells showed high levels of aneuploidy with modal number ~86, suggestive of a hypo-tetraploid status (Fig 2.7c). Taken together, these results suggest that overexpression of Telomerase perturbs the mechanism that regulate cellular ploidy in HT1080, and therefore confers chromosomal instability in these cells (CIN) - a hallmark of cancer progression in >90% of cancer cells in epithelial origin (Thompson and Compton, 2008).

8. Basal level of Damage is comparable for HT1080 and ST-HT1080 cells

Since ST-HT1080 cells are hypo-tetraploid (84-86 chromosomes) compared to HT1080 cells, we hypothesized that the basal levels DNA damage are potentially higher in these cells (Janssen et al., 2011). We determined the levels of 53BP1 foci at the single cell level by immunofluorescence and counted the number of 53BP1 foci per nuclei in both the cell lines.

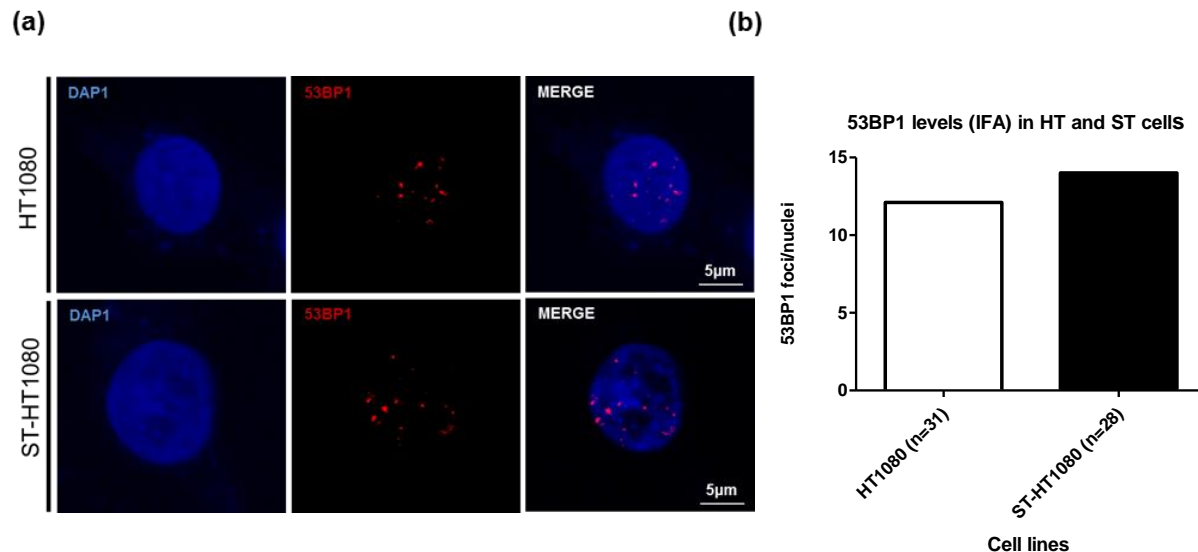
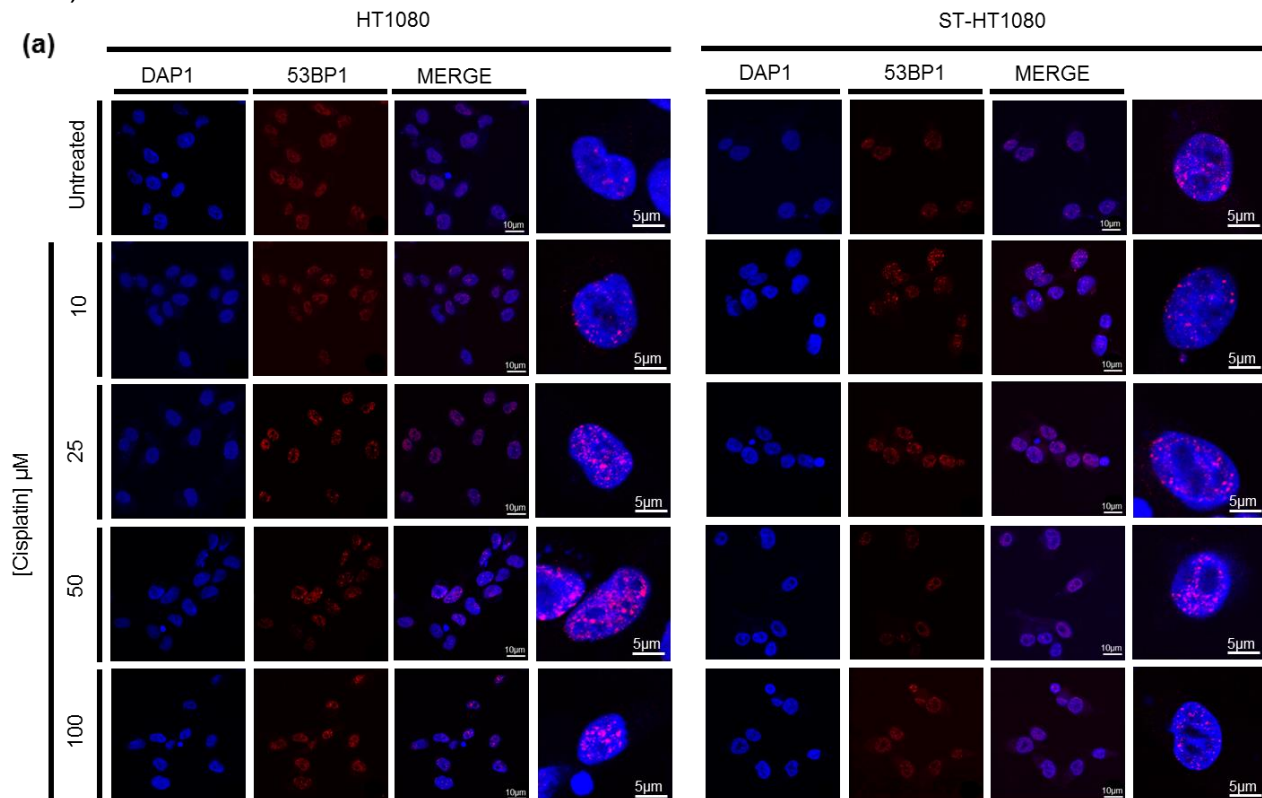


Figure 2.8: 53BP1 staining and quantification in HT1080 and ST-HT1080. (a) Representative zoomed in image of single nuclei of HT1080 and ST-HT1080 (b) Quantification of 53BP1 foci per nuclei in HT1080 (12) and ST-HT1080 (14), n= number of nuclei.

Contrary to our hypothesis, even though ST-HT1080 cells were polyploid, the basal levels of damage were comparable to HT1080 cells. While HT1080 has an average of 12 53BP1 foci per nucleus, ST-HT1080 cells have 14 foci (Fig 2.8). Even though highly aneuploid, ST cells do not show significantly different levels of 53BP1 foci as compared to HT1080 cells.

9. Effect of Cisplatin dose response on HT1080 and ST-HT1080 cells.

Assessment of basal levels of DNA damage using 53BP1 suggests comparable levels of damage between HT1080 and ST-HT1080 cells even though ST1080 cells have twice the DNA content as compared to HT1080 cells (Fig 2.7). We enhanced basal levels of DNA damage in these cells by using a well-known DNA damaging agent- Cisplatin (Sedletska et al., 2005) to examine if the extent of DNA damage is affected in cells that overexpress Telomerase i.e. in both HT1080 and ST-HT1080 cells. We stained for 53BP1, 3 hours after the addition of Cisplatin (0, 10, 25, 50 and 100 μM) (Fig 2.9).



(b)

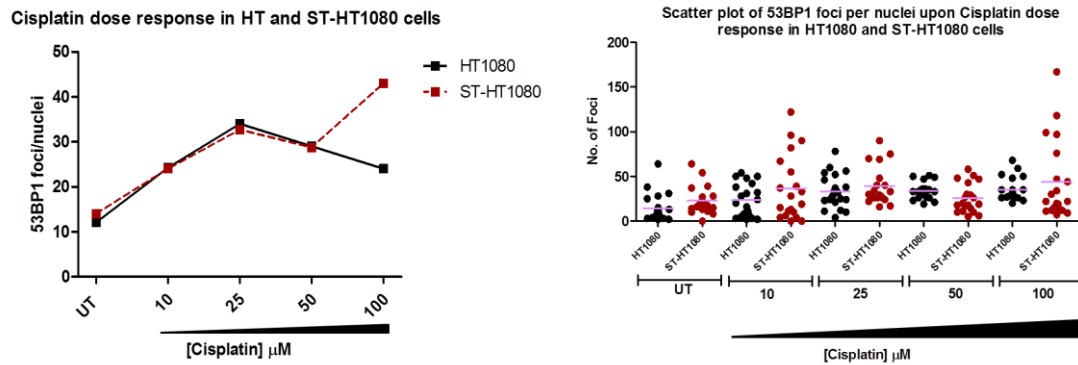


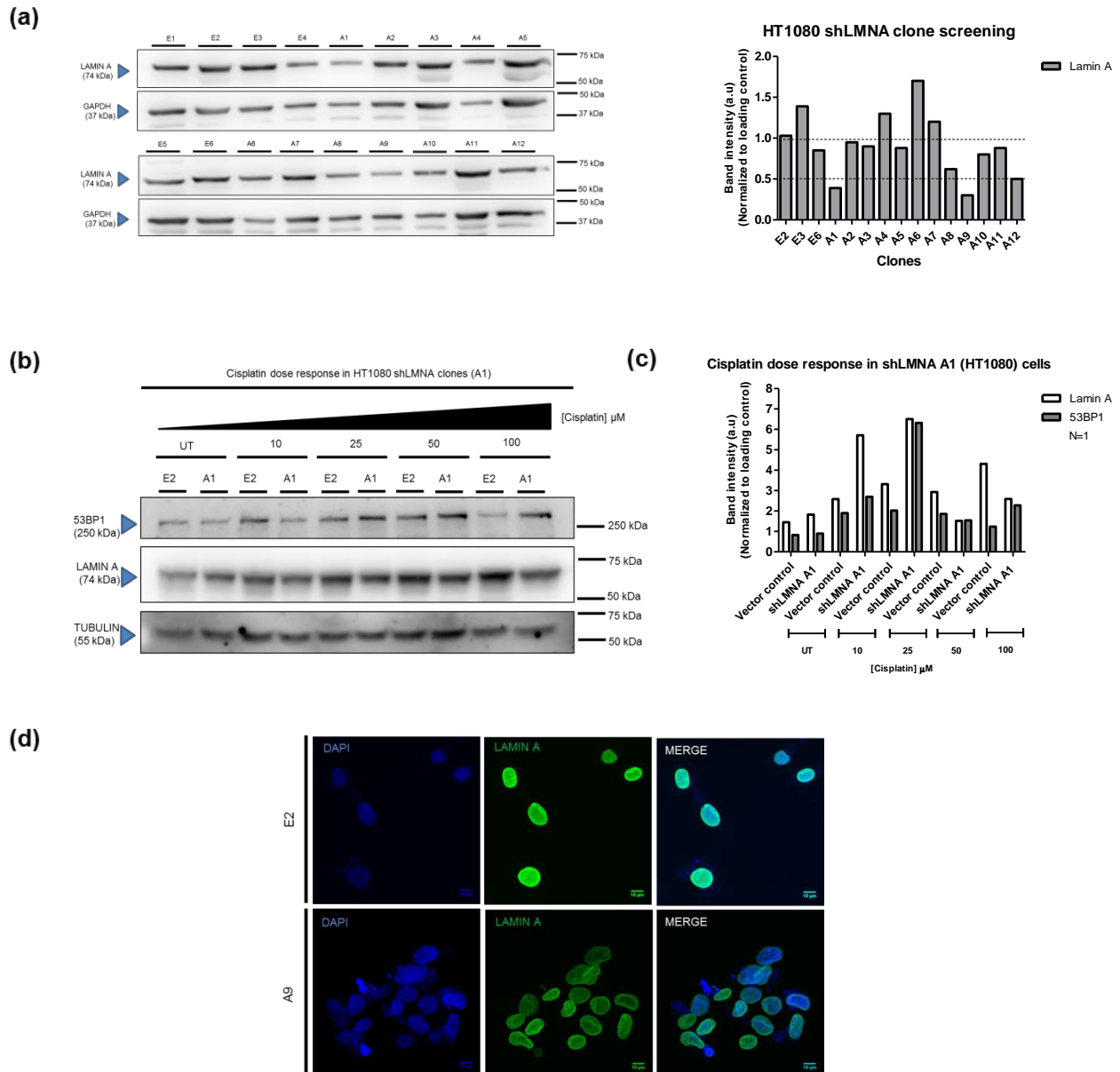
Figure 2.9: Cisplatin dose response in HT1080 and ST-HT1080. (a) Representative images of 53BP1 foci in HT1080 cells (left) and ST-HT1080 cells (right) (b) Quantification of the 53BP1 foci per nuclei upon Cisplatin treatment in HT1080 and ST-HT1080 cells. Number of nuclei: UT (HT-31, ST-28), 10 µM (HT-27, ST-35), 25 µM (HT-33, ST-34), 50 µM (HT-33, ST-33), 100 µM (HT-31, ST-33) (c) Scatter plot depicting the average number of 53BP1 foci per nucleus across increasing dose of Cisplatin (n=20 for each set)

Interestingly Cisplatin dose response is similar in both the cell lines. Till 25 µM, both the cell lines showed a dose response with 53BP1 foci per nuclei for HT1080 cells being 12, 24 and 34 and that for ST-HT1080 cells being 14, 24 and 32 for UT, 10 and 25 µM respectively. Mean values from the scatter plot are 14, 23, 33, 33 and 35 for HT1080 and 22, 36, 39, 25 and 43 for ST cells across treatments (Fig 2.9-b). However, the foci formation is non-linear beyond 25 µM indicating saturation in 53BP1 foci levels in HT1080 cells. However, in ST-HT1080 cells, dose response showed an increase in foci numbers at 100 µM (Fig 2.9-b). These foci numbers are derived from a single experiment and are being repeated across multiple independent biological replicates.

10. Lamin A depletion in HT1080 cells aggravates the Cisplatin dose response

We next examined whether depletion of Lamin A in HT1080 has a bearing on the 53BP1 foci formation. Studies in Mouse Embryonic Fibroblasts show that depletion of Lamin A reduces the levels of 53BP1 and there by affects the DNA damage response post IR irradiation (Redwood et al., 2011). We therefore examined the effect of Lamin depletion in HT1080 cells. We downregulated Lamin A levels by transfecting HT1080 cells with shRNA against Lamin A for 48 hours followed by stable selection of clones

using puromycin treatment (400 ng/ml). Continuous selection for over 7 days enabled us to derive two independent stable clones (A1 and A9). Western blot analysis of extracts prepared from these clones showed ~65% downregulation of Lamin A (Fig 2.10a). Cisplatin dose response was carried out in both clones A9 (IFA) and A1 (WB) (Fig 2.10a-g).



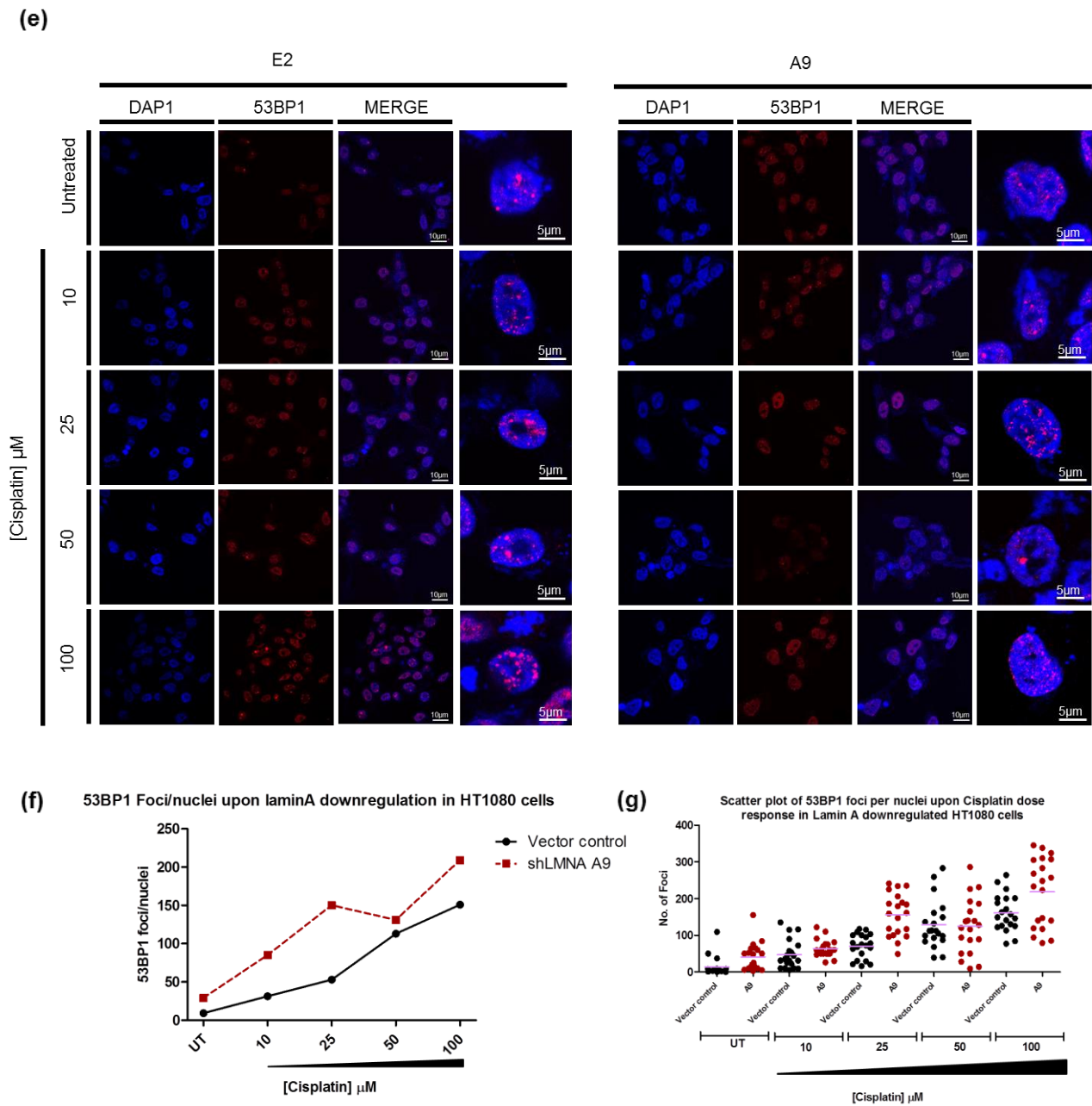
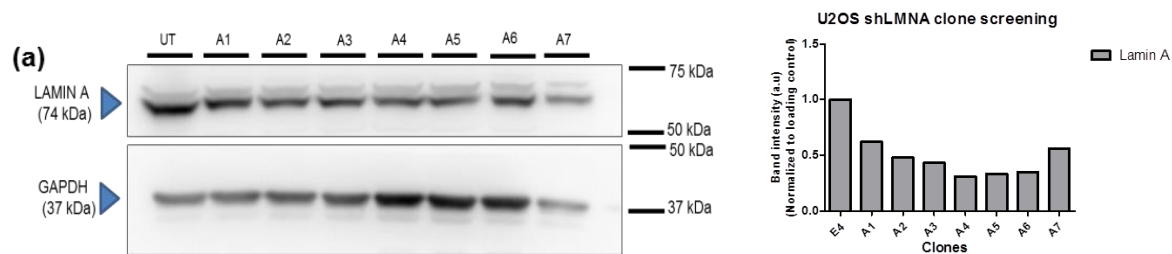


Figure 2.10: Cisplatin dose response in Lamin A depleted HT1080 cells (a) Western blots representing HT1080 shLMNA clone screening (b) Western blot representing the Cisplatin dose response in shLMNA A1 clone (c) Quantification of the blots with respect to loading control Tubulin (d) Representative images of Z-projected nuclei of the vector control (first panel) and shLMNA A9 clone (second panel) indicating levels of Lamin A in both (e) Representative images of 53BP1 staining in Vector control (left) and shLMNA A9 cells (right) (f) Quantification of the 53BP1 foci per nuclei upon Cisplatin treatment in Vector control and shLMNAA9 cells. Number of nuclei: UT (VC-46, A9-47), 10 μM (VC-47, A9-47), 25 μM (VC-50, A9-40), 50 μM (VC-39, A9-38), 100 μM (VC-62, A9-56). (g) Scatter plot depicting the average number of 53BP1 foci per nucleus across different doses of Cisplatin (n=20 for each set)

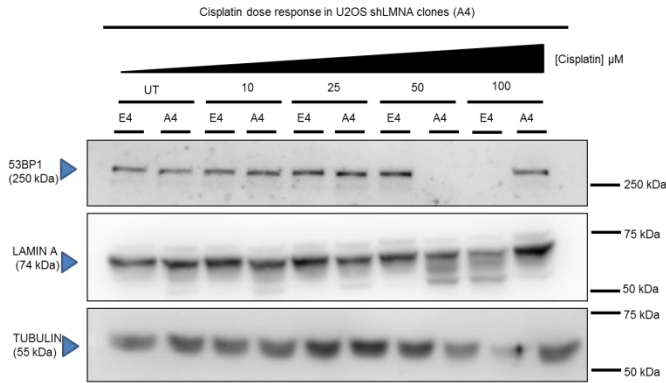
Clone A1 shows a partial Lamin A downregulation, it is important to note that 53BP1 levels show an increase specifically upon Lamin A down regulation as compared to the cells transfected with vector control (Fig 2.10b). The decrease in Lamin A levels was further evident in an independent stable clone A9, at the single cell level (Fig 2.10d) as compared to the vector control (E2). Lamin A downregulation in HT1080 showed enhanced 53BP1 foci induced by Cisplatin as compared to the vector control (Fig 2.10e, f). Quantification of the same reveal that Lamin A downregulated cells are much more sensitive to DNA damage and hence show increasing numbers of 53BP1 foci/nuclei (29, 85, 150, 131 and 209) compared to that of vector control (9, 31, 53, 113 and 151) for Cisplatin concentrations tested. Mean values from the scatter plot are 13, 47, 70, 128 and 161 for vector control and 41, 63, 155, 124 and 218 for shLMNA A9 cells. The foci numbers have been aggregated from single experiment. Data is being compiled from multiple independent experiments.

11. Lamin A depletion in U2OS cells hampers the Cisplatin dose response

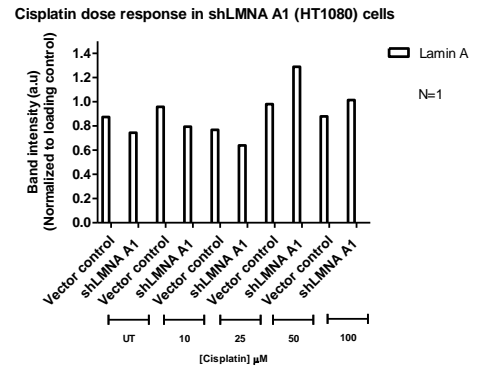
Lamin A down regulation in a fibrosarcoma cell line enhanced cisplatin dose response resulting in an increase in DNA damage induced 53BP1 foci (Fig 2.10e, f). We wanted to examine if U2OS cells shows a response comparable or independent to that of HT1080 cells. Lamin A was downregulated in U2OS by shRNA transfection. Cells were subjected to puromycin selection (400 ng/ml) in order to select for stable Lamin A knockdown clones. A single clone was derived (A4), which showed ~65% downregulation in Lamin A at the population level compared to other clones (Fig 2.11a). We followed up shLMNA clone A4 to ascertain the effect of Cisplatin treatment at the population as well as at the single cell level (Fig 2.11a-g).



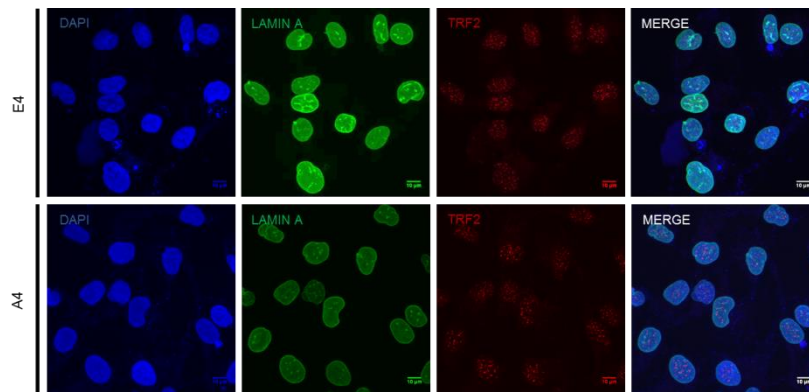
(b)



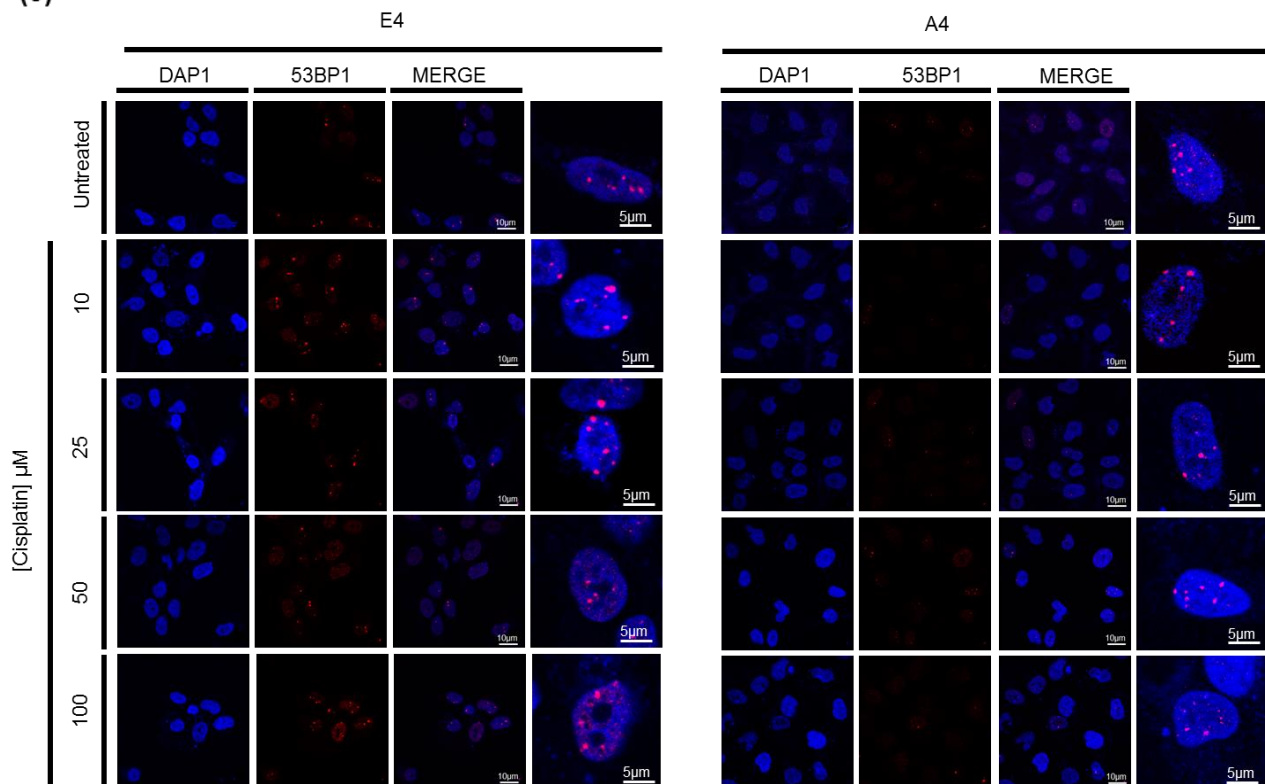
(c)



(d)



(e)



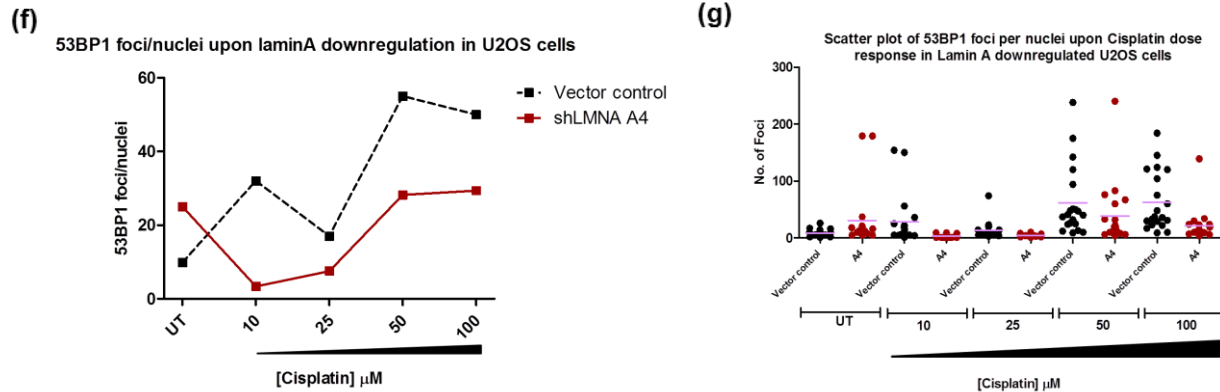


Figure 2.11: Cisplatin dose response in Lamin A depleted U2OS cells (a) Western blots representing shLMNA clonal screening (b) Western blots the Cisplatin dose response in shLMNA A4 clone (c) Quantification of the Lamin A blots with respect to loading control Tubulin (d) Representative images of Z-projected nuclei of the vector control (E4, first panel) and shLMNA A4 clone (second pane) indicating levels of Lamin A in both. TRF2 foci are also shown (e) Representative images of 53BP1 staining in Vector control (left) and shLMNA A4 cells (right) (f) Quantification of the 53BP1 foci per nuclei upon Cisplatin treatment in Vector Control (VC) and shLMNA A4 cells. Number of nuclei: UT (VC-46, A4-50), 10 μM (VC-56, A4-47), 25 μM (VC-47, A4-51), 50 μM (VC-49, A4-49), 100 μM (VC-53, A4-52) (g) Scatter plot depicting the average number of 53BP1 foci per nucleus across different doses of Cisplatin (n=20 for each set).

Western blot showed a decrease in Lamin A levels in shLMNA A4 cells as compared to the vector control and an increase in 53BP1 levels upon cisplatin dose (E4) (Fig 2.11a). At the single cell level, clone A4 showed reduced Lamin A compared to the vector control (Fig 2.11d). Cisplatin dose response in Lamin A downregulated U2OS cells displayed a phenotype which is completely different when compared to Lamin A downregulated HT1080 cells. While in HT1080 cells, downregulation of Lamin A led to an increase in 53BP1 foci, in U2OS cells this led to a decrease in 53BP1 foci number (Fig 2.11e, f). Quantification of the same revealed that 53BP1 foci number/nuclei in shLMNA A4 clones are 25, 3, 7, 28 and 29; while in vector control the values are comparatively higher at 9, 32, 17, 55 and 50 foci for untreated, 10, 25, 50 and 100 μM treatments respectively (Fig 2.11-e). Mean values from the scatter plot are 8, 28, 13, 61 and 62 for vector control and 30, 3, 4, 38 and 21 for shLMNA A4 cells. 53BP1 foci numbers in this experiment have been aggregated from single experiment. Data is being compiled from multiple independent experiments.

12. Lamin A downregulated cells show fewer large foci upon DNA damage induction

HT1080 and U2OS cells stained for 53BP1 in which Lamin A is downregulated revealed an interesting phenotype. In both the cell lines, the mean volume of the 53BP1 foci formed is considerably less in the shLMNA clones compared to their respective vector controls (Fig 2.10e, Fig 2.11e). Since Lamin A affects the positional stability of γ -H2AX foci during DNA damage induction (Mahen et al., 2013), we tested whether down regulation of Lamin A affects the relative volume of 53BP1 foci formed. We analyzed the 53BP1 foci volumes using Huygens Professional software in shLMNA clones (A9 and A4) of HT1080 and U2OS with respect to their respective vector controls (Fig 2.12a, b)

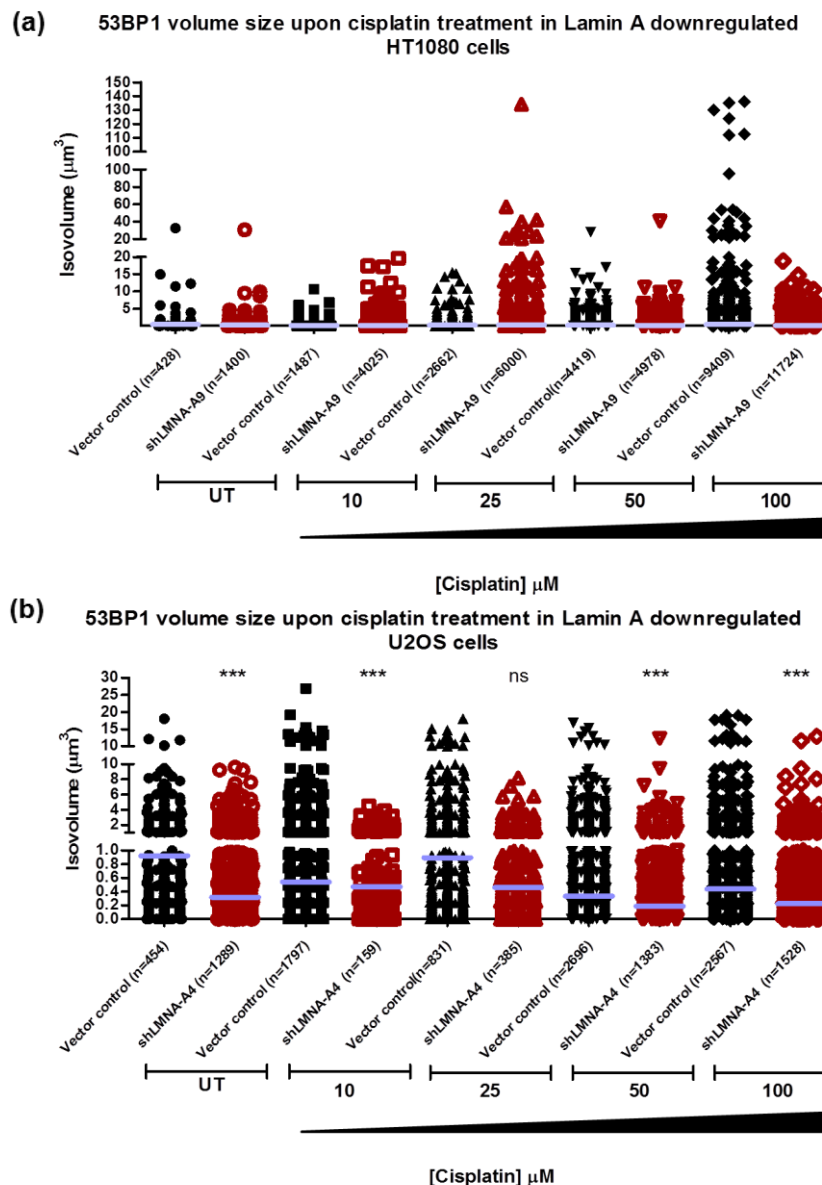


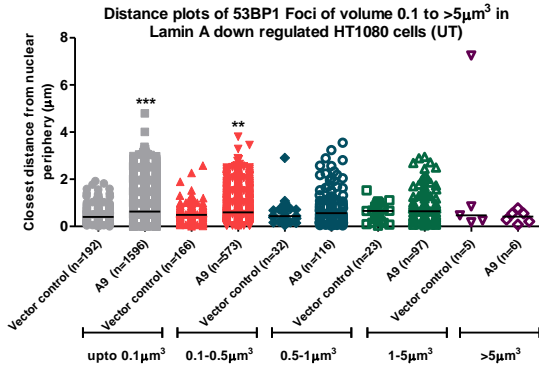
Figure 2.12: 53BP1 foci volume upon cisplatin treatment in Lamin A down regulated HT1080 and U2OS cells. (a) Graph depicting volume range and mean volume (purple bar) of 53BP1 foci formed upon Cisplatin treatment in shLMNA clone A9 (HT1080) and respective Vector control. (b) Graph depicting volume range mean volume (purple bar) of 53BP1 foci formed upon Cisplatin treatment in shLMNA clone A4 (U2OS) and respective Vector control, (n = number of foci analyzed ns: p>0.05, *: p<0.05, **: p<0.01, *: p<0.001)**

Mean volume of 53BP1 foci in Lamin A downregulated HT1080 cells are 0.22, 0.15, 0.33, 0.18 and 0.14 μm^3 compared to 0.44, 0.13, 0.20, 0.20 and 0.38 μm^3 of Vector control for UT, 10, 25, 50 and 100 μM treatments respectively (Fig 2.12-a). Even though not significant at 50 and 100 μM treatments, number of large foci formed ($>10 \mu\text{m}^3$) is considerably lower in shLMNA A9 compared to vector control (Fig 2.12-a). In U2OS cells, the difference in mean volume of 53BP1 foci between shLMNA A4 and vector control is more evident (Fig 2.12-b). While mean volume of 53BP1 foci in Lamin A downregulated U2OS cells are 0.31, 0.47, 0.46, 0.18 and 0.22 μm^3 for UT, 10, 25, 50 and 100 μM treatments respectively, the same values for vector controls are 0.92, 0.54, 0.89, 0.33 and 0.43 μm^3 (Fig 2.12b). This data implies a scaffolding role of Lamin A in building up 53BP1 at the damage site for robust signaling towards DNA repair proteins.

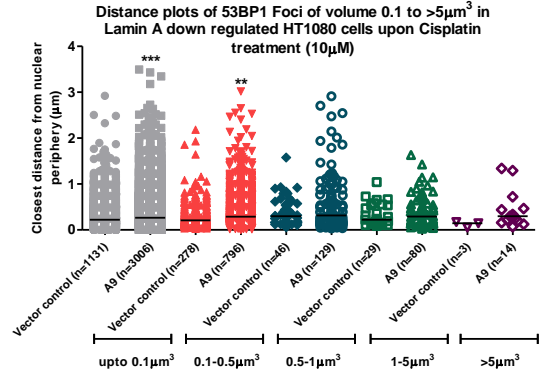
13. 53BP1 foci are formed proximal to the nuclear envelope in Lamin A depleted cells

Since Lamins interact with chromatin mainly via Lamin associated domains (LAD's) enriched towards the nuclear periphery and further are characterized by inactive histone marks (H3K9me2/me3) (Kind and van Steensel, 2010), we examined if Lamin A down regulation affects the extent of 53BP1 foci formation towards the nuclear periphery as the chromatin de-condenses due loss of tethering upon Lamin depletion. We quantified the shortest distance from individual foci to the nuclear periphery demarcated by DAPI staining (Shachar et al., 2015) in Lamin A downregulated HT1080 cells and U2OS cells (Fig 2.13a, b).

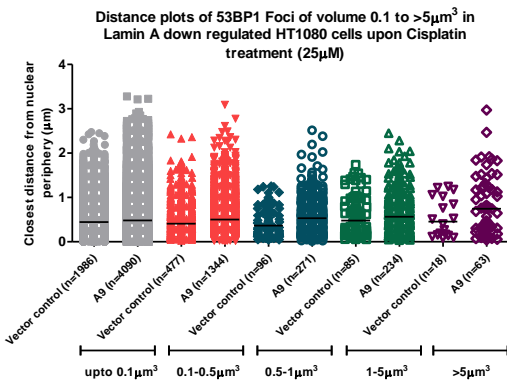
(a[1])



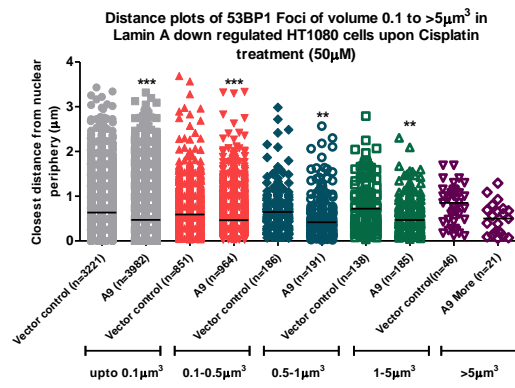
(a[2])



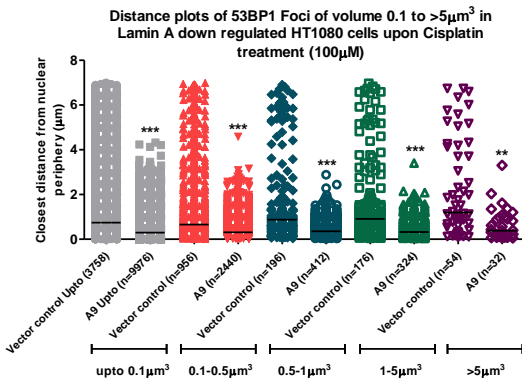
(a[3])



(a[4])

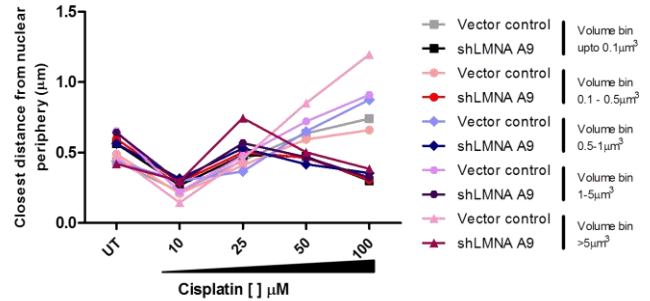


(a[5])

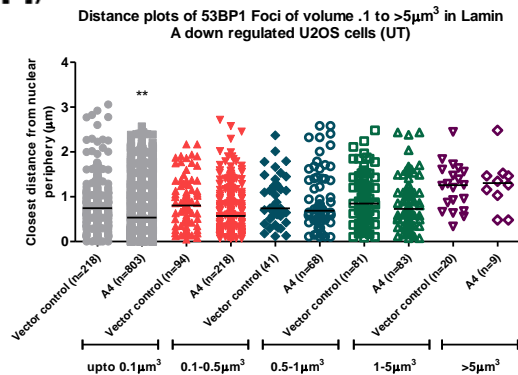


(a[6])

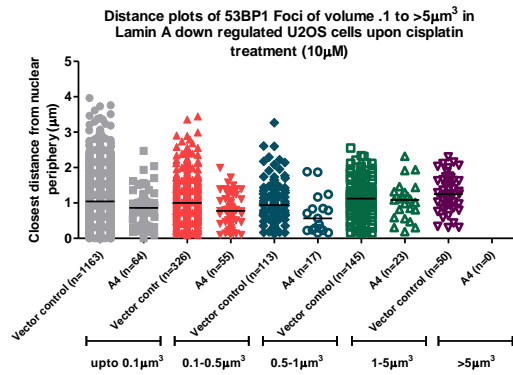
Median distance plot of 53BP1 foci of volume range 0 to >5µm³ in HT1080 cells depleted of Lamin A



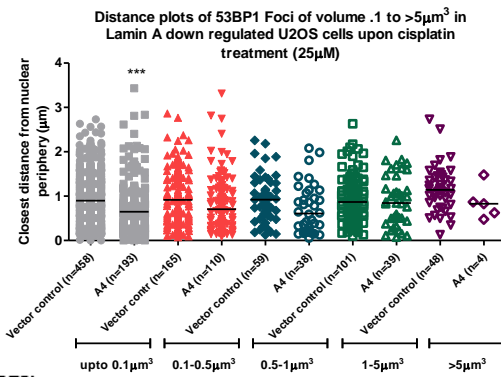
(b[1])



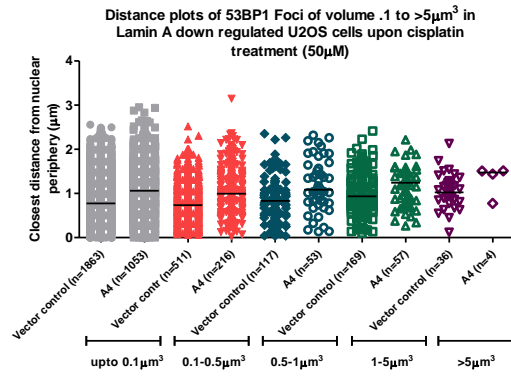
(b[2])



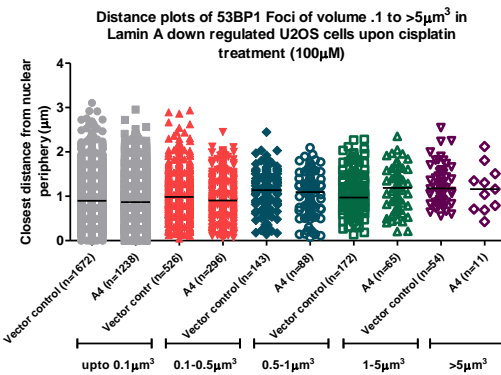
(b[3])



(b[4])



(b[5])



(b[6])

Median distance plot of 53BP1 foci of volume range 0 to >5µm³ in U2OS cells depleted of Lamin A

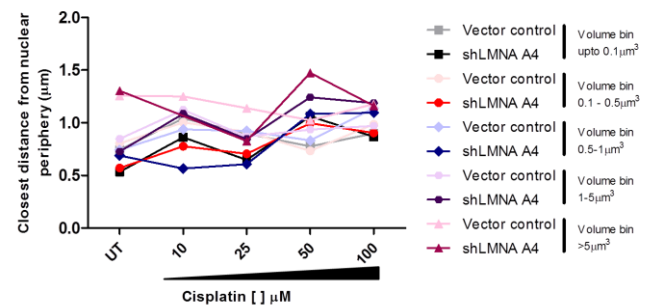


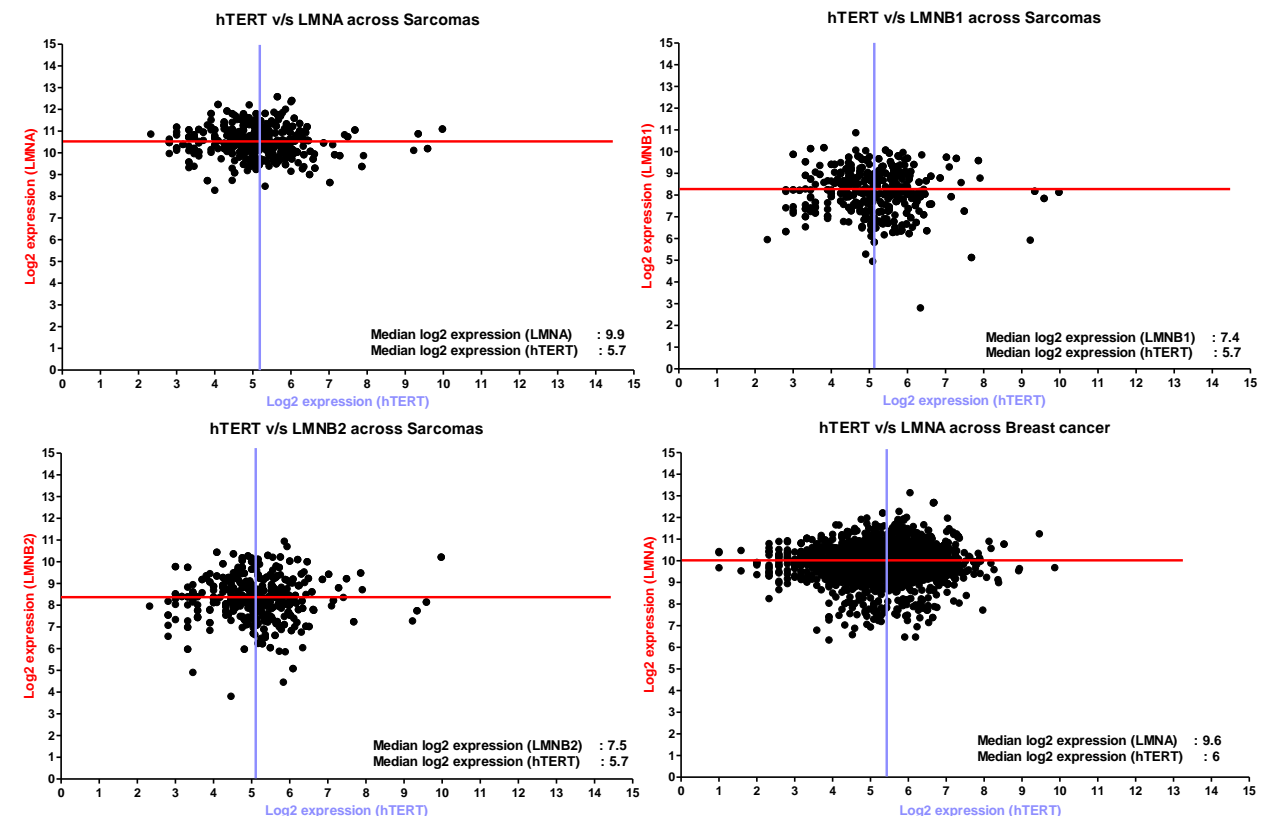
Figure 2.13: Median distance plots of 53BP1 foci of different volumes from the nuclear Lamina in Lamin A down regulated HT1080 and U2OS cells (a[1-5]) Median distance plots of 53BP1 foci of volume range 0.1 to >5µm³ across 0 (a-1), 10 (a-2), 25 (a-3), 50 (a-4) and 100 (a-5) cisplatin treatments in Lamin A downregulated HT1080 cells (shLMNA A9) (a-6) Line graphs combining median distances across treatments for all the volume bins (b-[1-5]) 0.1 to >5µm³ across 0 (b-1), 10 (b-2), 25 (b-3), 50 (b-4) and 100 (b-5) cisplatin treatments in Lamin A downregulated U2OS cells (shLMNA A4) (a-6) Line graphs combining median distances across treatments for all the volume bins in U2OS cells.

The volumes of the 53BP1 foci were sorted into 5 bins (0-0.1µm³, 0.1-0.5µm³, 0.5-1µm³, 1-5µm³ and >5µm³) across Cisplatin treatments and median distances from the nuclear border for each bin was plotted against controls. In HT1080, median distance is similar across bins between shLMNA A9 and vector control for UT, 10 and 25 µM (Fig 2.13a[1-5]). However, for 50 and 100µM, across all volume bins, the median significantly changed and foci were more peripheral in shLMNA depleted cells compared to control (Fig 2.13a[4,5,6]). In U2OS cells (shLMNA A4), the 53BP1 foci is more peripheral across volume bins of 1µm³ for UT, 10 and 25 µM treatments compared to vector controls (Fig 2.13-b[1-3]). Foci of volume above 1µm³ are largely internal for the above

mentioned conditions. At 100 μM , foci of volume till volume range $1.0 \mu\text{m}^3$ to $>5.0 \mu\text{m}^3$ formed, have a median distance identical to that of control cells. Taken together the data implies more enrichment of 53BP1 foci upon DNA damage at the periphery in Lamin A downregulated cells compared to the vector controls.

14. Patient data reveal cases of High Telomerase and low Lamin Levels

We next examined Gene expression across Normal and Tumor Tissue (GENT) database to examine if a potential correlation exists between Lamins and NHEJ factors with hTERT in patient samples (Fig 3.1, 3.2). Comparative expression analysis of solid tumors (Sarcomas, Breast cancers) and Leukemias reveals that B-type Lamins are downregulated compared to Lamin A (Fig 3.1). To check if a correlation exists between hTERT overexpression and Lamins, we analyzed subsets of data with hTERT levels higher than the population median (right of violet line). Interestingly, Lamin B1 and B2 levels plotted from the same data sets indicate that in ~45% of population where hTERT expression is high, Lamin B1 and B2 levels are lower across cancers in comparison to Lamin A levels.



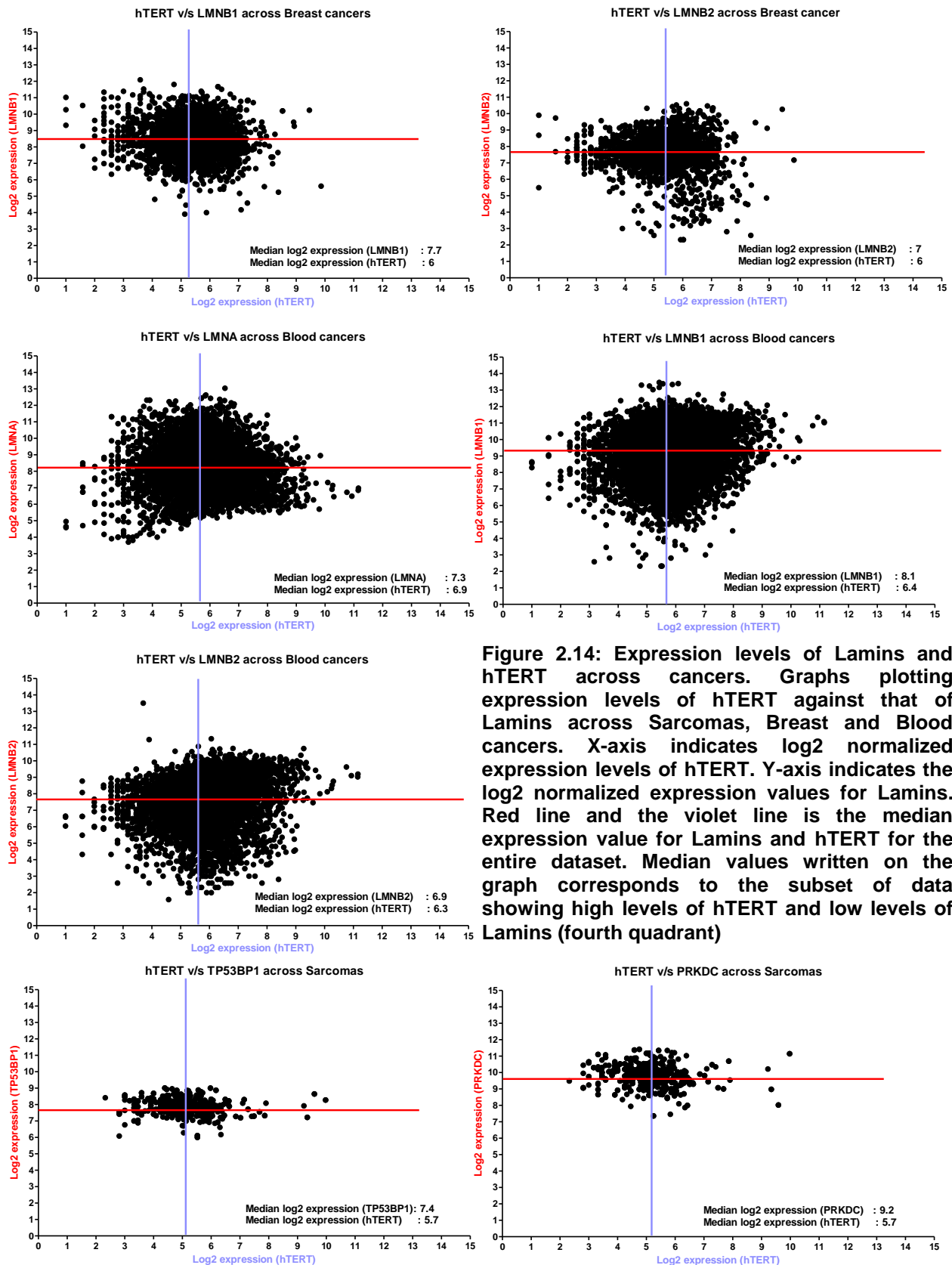
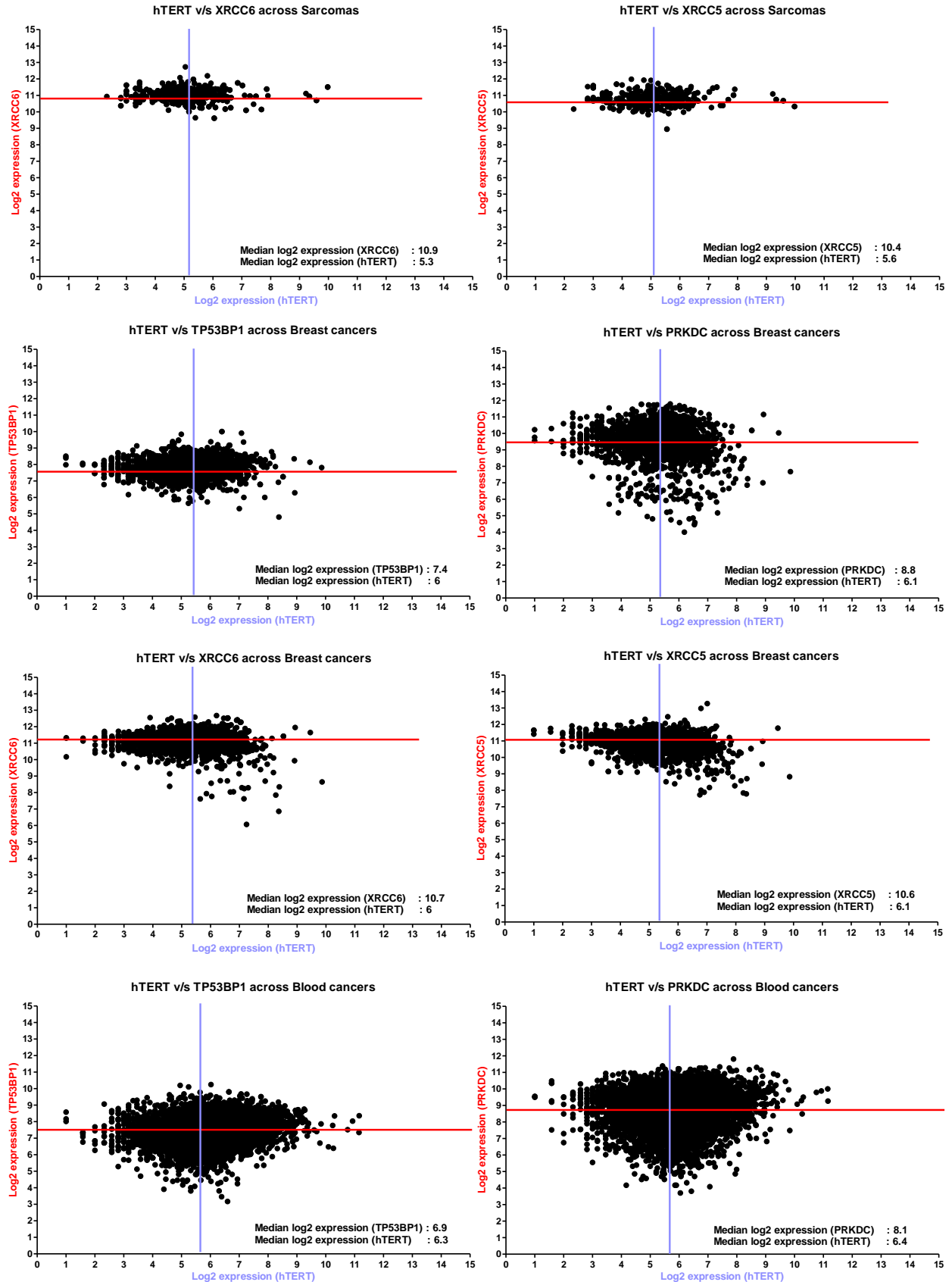


Figure 2.14: Expression levels of Lamins and hTERT across cancers. Graphs plotting expression levels of hTERT against that of Lamins across Sarcomas, Breast and Blood cancers. X-axis indicates log2 normalized expression levels of hTERT. Y-axis indicates the log2 normalized expression values for Lamins. Red line and the violet line is the median expression value for Lamins and hTERT for the entire dataset. Median values written on the graph corresponds to the subset of data showing high levels of hTERT and low levels of Lamins (fourth quadrant)



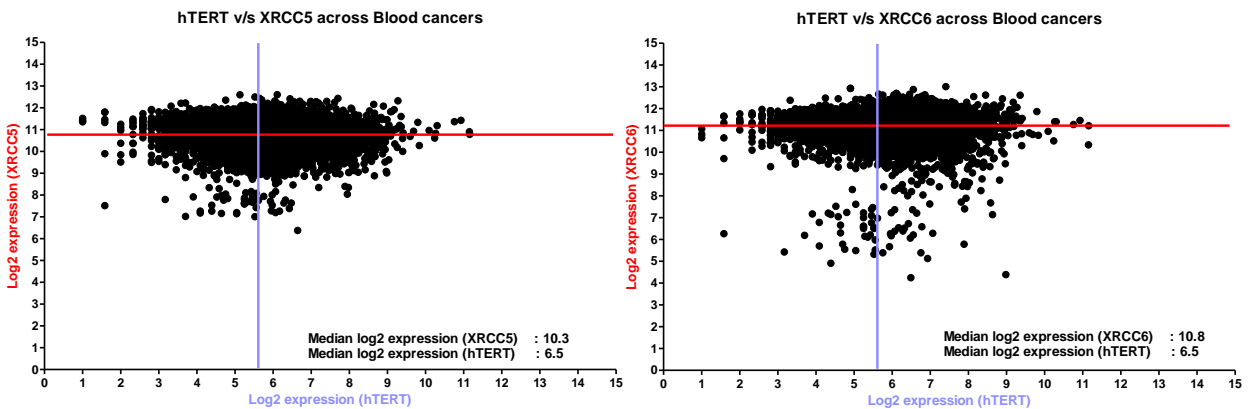


Figure 3.2: Expression levels of NHEJ regulators and hTERT across cancers. Graphs showing expression levels of hTERT against TP53BP1 (53BP1), PRKDC (DNA-PKcs), XRCC5 (KU80) and XRCC6 (KU70) across Sarcomas, Breast and Blood cancers. X-axis: log2 normalized expression levels of hTERT. Y-axis: log2 normalized expression value for NHEJ factors. Red line and the violet line is the median expression value for respective NHEJ molecules and hTERT for the entire dataset. Median values correspond to the subset of data showing high levels of hTERT and low levels of Lamins (Fig 3.2, fourth quadrant)

Comparison between levels of hTERT and NHEJ regulators in these cancers reveal that in the population with high hTERT expression, levels of 53BP1 and DNA-PKcs is relatively lower compared to KU proteins.

DISCUSSION

Recent studies increasingly provide evidence for the role of Lamin A in DNA damage response. Lamin A imparts positional stability to γ -H2AX during damage induction (Mahen et al., 2013) and stabilizes levels of 53BP1 - a major regulator of DNA repair pathway, checkpoint signaling as well as synapsis of distal DNA end during NHEJ (Gibbs-Seymour et al., 2015; Panier and Boulton, 2014). Lamin A downregulation in MCF7 cells resulted in impaired HR mediated repair because of partial transcriptional repression of key molecules such as BRACA1 and RAD51. Lamin A deficient cells are sensitive to DNA damaging agents such as Cisplatin that cause interstrand cross-links. Interestingly at the other end of the spectrum, ALT positive cells that ectopically expressed telomerase tolerate genomic insults induced by Etoposide and platinating agents such as Oxaloplatins (Fleisig et al., 2016). Therefore, we considered it relevant to test whether Telomerase overrides DNA damage induced by the depletion of Lamin A.

We tested our hypothesis in cell lines with varying levels of Telomerase. We selected HT1080 (Fibrosarcoma), ST-HT1080 (stably overexpressing Telomerase) and a Telomerase negative cell line U2OS (Osteosarcoma). U2OS cells maintain Telomere length through ALT mechanism (Henson et al., 2005). We characterized the basal levels of Lamins, hTERT, and 53BP1 with an aim to examine their regulatory cross talk in DNA damage response. Compared to HT1080 cells, ST-HT1080 cells showed reduced levels of B-type Lamins, while Lamin A levels were comparable (Fig 2.1-a, b). ST-HT1080 cells expressed detectable amount of hTERT, while both HT1080 and U2OS cells show hardly any expression, consistent with previous reports that the endogenous expression of hTERT is undetectable upon immunoblotting (Xi and Cech, 2014). In contrast, 53BP1 levels are relatively higher in HT1080 cells compared to other cell lines that we tested. RT-PCR analysis revealed a transcriptional down regulation of B-type Lamins in HT1080 cells (Fig 2.2-a). In U2OS cells, B-type lamins are robustly expressed compared to HT1080. This led us to test if hTERT regulates levels of B-type Lamins. We examined transcript levels of Lamins and hTERT across cancer cell lines (Fig 2.3). Real time PCR analysis largely revealed an inverse relationship between B-

type Lamin levels and hTERT. It is unclear if relative stoichiometric differences between Lamin levels across cell types (Guo et al., 2014) have a feedback effect in maintaining such an inverse relationship between low Lamins and high Telomerase transcript levels. Recent studies using super-resolution microscopy suggests that Lamin A/C shows a distinct organization and structure that stabilizes the nuclear lamina, distinct from Lamin B2 that further corroborates the non-overlapping roles of A and B-type Lamins in nuclear organization and function (Shimi et al., 2015; Swift et al., 2013). Even though one could speculate that Lamin B1 is more sensitive to Telomerase levels, further experimental validation is required.

Patient data also showed a significant number of cases (~25% of the entire population) where the levels of hTERT were much higher than the population median while the levels of B-type lamins were lower than that of the population median (Fig 2.14). DNA-PKcs expression is lower in subsets of patient data where hTERT expression is high. It is pertinent to note that Lamin B1 downregulation leads to reduced levels of DNA-PKcs (Butin-Israeli et al., 2015). KU proteins are highly overexpressed in those subsets across cancers that were considered.

We surmise that since HT1080 cells show endogenous Telomerase expression, Lamin levels may be insensitive to transient upregulation of Telomerase in contrast to the effect on U2OS cells (Fig 2.4). Down regulation of Lamins might be a sequential event setting in after prolonged exposure to elevated levels of telomerase. Generating stable hTERT overexpressing clones would confirm the hypothesis. We also ascertained that effect of Lamin downregulation is independent of Telomerase function for telomere maintenance in U2OS cells and is an extra-telomeric role of Telomerase (Fig 2.5).

Transcription Factor overlap between Lamins

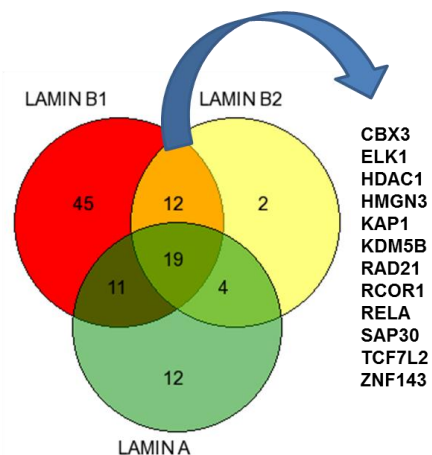


Figure 3.1: Transcription factor overlap between the promoters of Lamin A, B1 and B2.

In order to dissect the mechanisms that regulate Lamin down regulation, we performed in-silico analysis of Transcription factors that are bound between 0-1 kbp upstream of Transcription Start Site (TSS) of Lamin promoters and examined the association of putative transcription factors with hTERT. Promoter analysis revealed 48, 89 and 40 transcription factor at Lamin A, B1 and B2 promoters respectively (Fig 3.3). Out of which B1 and B2 showed 12 Transcription factors in common. We analyzed whether any of the listed factors interact with hTERT. Interestingly, nuclear factor NF-kappa-Bp65 subunit or RELA shows an association as determined BIOGRID interaction analyses, which is an important effector in the NF-kB signaling pathway (Vallabhapurapu and Karin, 2009). Literature survey also corroborates a direct interaction, in which hTERT directly recruits RELA to NF-kB target genes that help in cell proliferation, invasion and apoptosis resistance (Ghosh et al., 2012). Recent studies reveals a novel complex formed by transcription factor YY1 and RELA which mediates transcriptional repression of the pro-apoptotic gene BIM in multiple myelomas that aids cell survival (Potluri et al., 2013). Since in-silico analyses reveals YY1 occupancy at Lamin promoter, we speculate a complex comprising hTERT-RELA-YY1 that represses expression of LMNB1 and LMNB2. CHIP-PCR will further validate the existence of this sub-complex.

Studies have shown that the nuclear stiffness scales with increase in Lamin A to B ratio; at the same time increased stiffness impedes 3D cell migration (Harada et al., 2014). Studies also show enhanced migration as well as proliferation upon Lamin A overexpression (Kong et al., 2012). Increase in nuclear stiffness, fashioned by increase in Lamin A to B ratio, may protect cells from stress induced DNA damage and there by apoptosis commonly observed in 3D migration of cells and thus giving an added advantage in migration.

Genomic insults on Telomerase overexpressing ALT+ cell lines (U2OS and VA13) results in cells that are 4n and subsequently 8n, suggesting a role for Telomerase in sustaining cells with greater tolerance for gross chromosomal instabilities (Fleisig et al., 2016). Cisplatin treatment on HT1080 and ST-HT1080 cells revealed comparable level of DNA damage in both these cell types having striking differences in ploidy (Fig 2.9). Depleting, Lamin A in HT1080 cells showed a significant increase in 53BP1 foci (Fig 2.10) as compared to controls, indicating that Lamin depletion renders HT1080 cells are

more prone to damage. Additionally, volume of 53BP1 foci is considerably lower than that of control cells at higher cisplatin doses consistent with U2OS cells downregulated of Lamin A (Fig 2.12). Lamins thus not only stabilize 53BP1 levels but may function as a scaffold that regulates 53BP1 foci volume along with γ -H2AX upon DNA damage. In contrast, U2OS cells showed a decrease in 53BP1 foci numbers upon Lamin A down regulation, consistent with previous studies (Fig 2.11) (Gibbs-Seymour et al., 2015).. Overexpressing Telomerase in Lamin A depleted cells would provide useful insights into regulation of DNA damage response. Along with a decrease in the volume of 53BP1 foci, the foci formed were proximal to the nuclear periphery as compared to controls (Fig 2.13). Lesions at the periphery of the nucleus are repaired via NHEJ (Lemaître et al., 2014), suggesting distinct hierarchies in DNA damage regulation proximal to the nuclear envelope. Our data suggests that Lamin A downregulation potentially converts the nuclear periphery to a DNA damage “hot spot”. As Lamin A levels are low, due to loss of tethering, Lamin A Associated Domains (LAD’s) open up and are more prone to DNA damage compared to the nuclear interior. Another possibility is an active migration of the damaged sites to the periphery for repair; however studies analyzing the dynamics of DSB’s negate this possibility as broken DNA does not show significant nuclear movement to the periphery (Soutoglou et al., 2007). Even though Lamin A downregulation increases the dynamics of the DSB (Mahen et al., 2013); Lamins function as a chromatin tether to limit DNA movement for efficient recruitment of repair proteins. Our data also suggests a threshold dependent function of Lamin A in the context of DNA damage. Since preliminary data suggests that Lamin A downregulation increases basal level of DNA damage in the system while hTERT has a protective role against damage, we propose that a careful analysis of the levels of hTERT and Lamins are of prognostic value as cells overexpressing Lamins and hTERT would be resistant to chemotherapeutics. Fig 3.4 summarizes the results obtained from the study.

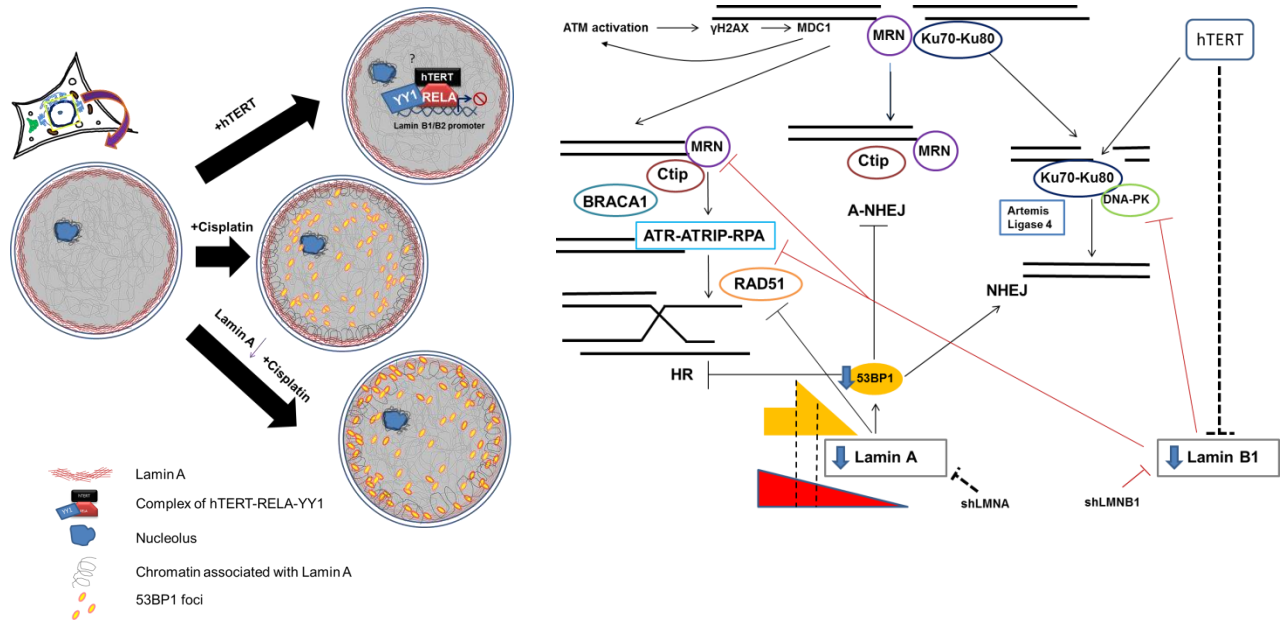
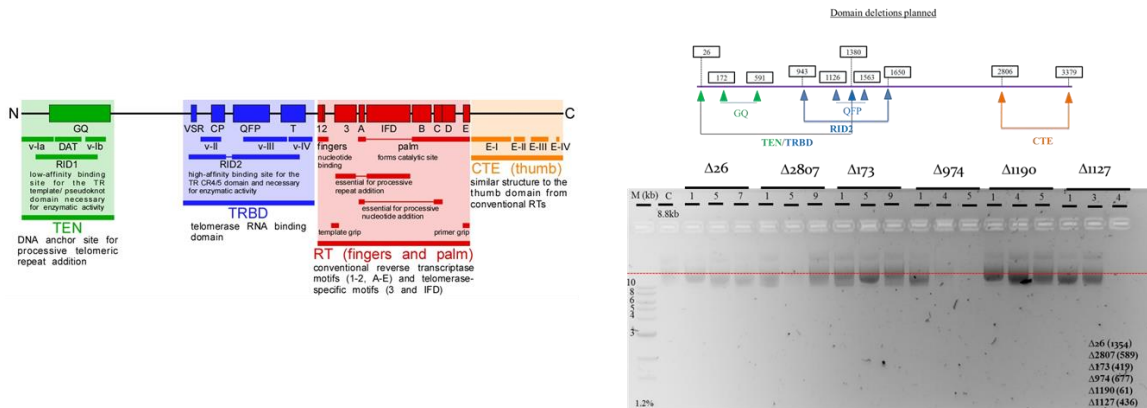


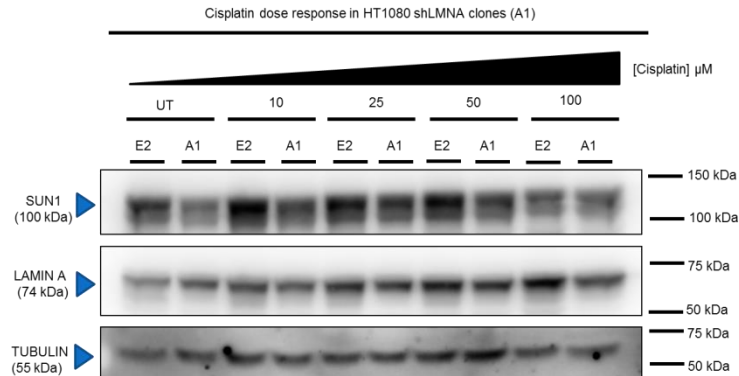
Figure 3.2: Schematic model depicting effect of hTERT overexpression, Lamin A downregulation in a model cell line. In the background of Lamin A downregulation upon DNA damage, more 53BP1 foci is formed at the nuclear periphery. Proposed roles of Lamin A hTERT and Lamin B1 in DNA damage response

Future Directions

- Since RID domain has been shown to be important for non-canonical role of Telomerase (Fleisig et al., 2016), make domain deletions of the enzyme and test which domain is responsible for the downregulation of B-type Lamins.



- Understand whether upon Lamin A downregulation, the decrease in SUN1 levels has any functional bearing on DNA damage response or Telomere position inside the nucleus (Lei et al., 2012).



- Overexpress Telomerase in shLMNA clones and assess the level of damage and organization of 53BP1 foci upon Cisplatin treatment.
- Downregulate Lamin A in ST-HT1080 and assess the level of damage and organization of 53BP1 foci.

References

- Batista, L.F., and Artandi, S.E. (2009). Telomere uncapping, chromosomes, and carcinomas. *Cancer Cell* 15, 455–457.
- Bothmer, A., Robbiani, D.F., Di Virgilio, M., Bunting, S.F., Klein, I.A., Feldhahn, N., Barlow, J., Chen, H.T., Bosque, D., Callen, E., et al. (2011). Regulation of DNA end joining, resection, and immunoglobulin class switch recombination by 53BP1. *Mol Cell* 42, 319–329.
- Brachner, A., and Foisner, R. (2011). Lamins reach out to novel functions in DNA damage repair. *Cell Cycle* 10, 3426.
- Bryan, T.M., Englezou, A., Dalla-Pozza, L., Dunham, M.A., and Reddel, R.R. (1997). Evidence for an alternative mechanism for maintaining telomere length in human tumors and tumor-derived cell lines. *Nat Med* 3, 1271–1274.
- Butin-Israeli, V., Adam, S.A., Jain, N., Otte, G.L., Neems, D., Wiesmüller, L., Berger, S.L., and Goldman, R.D. (2015). Role of lamin b1 in chromatin instability. *Mol Cell Biol* 35, 884–898.
- Cao, K., Blair, C.D., Faddah, D.A., Kieckhafer, J.E., Olive, M., Erdos, M.R., Nabel, E.G., and Collins, F.S. (2011). Progerin and telomere dysfunction collaborate to trigger cellular senescence in normal human fibroblasts. *J Clin Invest* 121, 2833–2844.
- Cao, X., Kong, C.M., Mathi, K.M., Lim, Y.P., Cacheux-Rataboul, V., and Wang, X. (2014). The use of transformed IMR90 cell model to identify the potential extra-telomeric effects of hTERT in cell migration and DNA damage response. *BMC Biochem* 15, 17.
- Court, R., Chapman, L., Fairall, L., and Rhodes, D. (2005). How the human telomeric proteins TRF1 and TRF2 recognize telomeric DNA: a view from high-resolution crystal structures. *EMBO Rep* 6, 39–45.
- Cremer, M., von Hase, J., Volm, T., Brero, A., Kreth, G., Walter, J., Fischer, C., Solovei, I., Cremer, C., and Cremer, T. (2001). Non-random radial higher-order chromatin arrangements in nuclei of diploid human cells. *Chromosome Res* 9, 541–567.
- Ding, Z., Wu, C.J., Jaskelioff, M., Ivanova, E., Kost-Alimova, M., Protopopov, A., Chu, G.C., Wang, G., Lu, X., Labrot, E.S., et al. (2012). Telomerase reactivation following telomere dysfunction yields murine prostate tumors with bone metastases. *Cell* 148, 896–907.
- Doksani, Y., and de Lange, T. (2014). The role of double-strand break repair pathways at functional and dysfunctional telomeres. *Cold Spring Harb Perspect Biol* 6, a016576.

Dorner, D., Gotzmann, J., and Foisner, R. (2007). Nucleoplasmic lamins and their interaction partners, LAP2alpha, Rb, and BAF, in transcriptional regulation. *FEBS J* 274, 1362–1373.

Draskovic, I., Arnoult, N., Steiner, V., Bacchetti, S., Lomonte, P., and Londoño-Vallejo, A. (2009). Probing PML body function in ALT cells reveals spatiotemporal requirements for telomere recombination. *Proc Natl Acad Sci U S A* 106, 15726–15731.

Fasching, C.L., Bower, K., and Reddel, R.R. (2005). Telomerase-independent telomere length maintenance in the absence of alternative lengthening of telomeres-associated promyelocytic leukemia bodies. *Cancer Res* 65, 2722–2729.

Fawcett, D.W. (1966). On the occurrence of a fibrous lamina on the inner aspect of the nuclear envelope in certain cells of vertebrates. *Am J Anat* 119, 129–145.

Fleisig, H.B., Hukezalie, K.R., Thompson, C.A., Au-Yeung, T.T., Ludlow, A.T., Zhao, C.R., and Wong, J.M. (2016). Telomerase reverse transcriptase expression protects transformed human cells against DNA-damaging agents, and increases tolerance to chromosomal instability. *Oncogene* 35, 218–227.

Ghosh, A., Saginc, G., Leow, S.C., Khattar, E., Shin, E.M., Yan, T.D., Wong, M., Zhang, Z., Li, G., Sung, W.K., et al. (2012). Telomerase directly regulates NF- κ B-dependent transcription. *Nat Cell Biol* 14, 1270–1281.

Gibbs-Seymour, I., Markiewicz, E., Bekker-Jensen, S., Mailand, N., and Hutchison, C.J. (2015). Lamin A/C-dependent interaction with 53BP1 promotes cellular responses to DNA damage. *Aging Cell* 14, 162–169.

Goldman, A.E., Maul, G., Steinert, P.M., Yang, H.Y., and Goldman, R.D. (1986). Keratin-like proteins that coisolate with intermediate filaments of BHK-21 cells are nuclear lamins. *Proc Natl Acad Sci U S A* 83, 3839–3843.

Gonzalez-Suarez, I., Redwood, A.B., Perkins, S.M., Vermolen, B., Lichtensztejn, D., Grotsky, D.A., Morgado-Palacin, L., Gapud, E.J., Sleckman, B.P., Sullivan, T., et al. (2009). Novel roles for A-type lamins in telomere biology and the DNA damage response pathway. *EMBO J* 28, 2414–2427.

Greider, C.W., and Blackburn, E.H. (1987). The telomere terminal transferase of *Tetrahymena* is a ribonucleoprotein enzyme with two kinds of primer specificity. *Cell* 51, 887–898.

Guo, Y., Kim, Y., Shimi, T., Goldman, R.D., and Zheng, Y. (2014). Concentration-dependent lamin assembly and its roles in the localization of other nuclear proteins. *Mol Biol Cell* 25, 1287–1297.

- Harada, T., Swift, J., Irianto, J., Shin, J.W., Spinler, K.R., Athirasala, A., Diegmiller, R., Dingal, P.C., Ivanovska, I.L., and Discher, D.E. (2014). Nuclear lamin stiffness is a barrier to 3D migration, but softness can limit survival. *J Cell Biol* 204, 669–682.
- Henson, J.D., Hannay, J.A., McCarthy, S.W., Royds, J.A., Yeager, T.R., Robinson, R.A., Wharton, S.B., Jellinek, D.A., Arbuckle, S.M., Yoo, J., et al. (2005). A robust assay for alternative lengthening of telomeres in tumors shows the significance of alternative lengthening of telomeres in sarcomas and astrocytomas. *Clin Cancer Res* 11, 217–225.
- Janssen, A., van der Burg, M., Szuhai, K., Kops, G.J., and Medema, R.H. (2011). Chromosome segregation errors as a cause of DNA damage and structural chromosome aberrations. *Science* 333, 1895–1898.
- Jaskelioff, M., Muller, F.L., Paik, J.H., Thomas, E., Jiang, S., Adams, A.C., Sahin, E., Kost-Alimova, M., Protopopov, A., Cadiñanos, J., et al. (2011). Telomerase reactivation reverses tissue degeneration in aged telomerase-deficient mice. *Nature* 469, 102–106.
- Kim, N.W., Piatyszek, M.A., Prowse, K.R., Harley, C.B., West, M.D., Ho, P.L., Coviello, G.M., Wright, W.E., Weinrich, S.L., and Shay, J.W. (1994). Specific association of human telomerase activity with immortal cells and cancer. *Science* 266, 2011–2015.
- Kind, J., and van Steensel, B. (2010). Genome-nuclear lamina interactions and gene regulation. *Curr Opin Cell Biol* 22, 320–325.
- Kong, L., Schäfer, G., Bu, H., Zhang, Y., Zhang, Y., and Klocker, H. (2012). Lamin A/C protein is overexpressed in tissue-invading prostate cancer and promotes prostate cancer cell growth, migration and invasion through the PI3K/AKT/PTEN pathway. *Carcinogenesis* 33, 751–759.
- Kudlow, B.A., Kennedy, B.K., and Monnat, R.J. (2007). Werner and Hutchinson-Gilford progeria syndromes: mechanistic basis of human progeroid diseases. *Nat Rev Mol Cell Biol* 8, 394–404.
- Kudlow, B.A., Stanfel, M.N., Burtner, C.R., Johnston, E.D., and Kennedy, B.K. (2008). Suppression of proliferative defects associated with processing-defective lamin A mutants by hTERT or inactivation of p53. *Mol Biol Cell* 19, 5238–5248.
- Lei, K., Zhu, X., Xu, R., Shao, C., Xu, T., Zhuang, Y., and Han, M. (2012). Inner nuclear envelope proteins SUN1 and SUN2 play a prominent role in the DNA damage response. *Curr Biol* 22, 1609–1615.
- Lemaître, C., Grabarz, A., Tsouroula, K., Andronov, L., Furst, A., Pankotai, T., Heyer, V., Rogier, M., Attwood, K.M., Kessler, P., et al. (2014). Nuclear position dictates DNA repair pathway choice. *Genes Dev* 28, 2450–2463.

- Lieber, M.R. (2010). The mechanism of double-strand DNA break repair by the nonhomologous DNA end-joining pathway. *Annu Rev Biochem* 79, 181–211.
- Mahen, R., Hattori, H., Lee, M., Sharma, P., Jeyasekharan, A.D., and Venkitaraman, A.R. (2013). A-type lamins maintain the positional stability of DNA damage repair foci in mammalian nuclei. *PLoS ONE* 8, e61893.
- Martínez, P., and Blasco, M.A. (2011). Telomeric and extra-telomeric roles for telomerase and the telomere-binding proteins. *Nat Rev Cancer* 11, 161–176.
- Nandakumar, J., Bell, C.F., Weidenfeld, I., Zaugg, A.J., Leinwand, L.A., and Cech, T.R. (2012). The TEL patch of telomere protein TPP1 mediates telomerase recruitment and processivity. *Nature* 492, 285–289.
- Panier, S., and Boulton, S.J. (2014). Double-strand break repair: 53BP1 comes into focus. *Nat Rev Mol Cell Biol* 15, 7–18.
- Peter, M., Kitten, G.T., Lehner, C.F., Vorburger, K., Bailer, S.M., Maridor, G., and Nigg, E.A. (1989). Cloning and sequencing of cDNA clones encoding chicken lamins A and B1 and comparison of the primary structures of vertebrate A- and B-type lamins. *J Mol Biol* 208, 393–404.
- Polo, S.E., and Jackson, S.P. (2011). Dynamics of DNA damage response proteins at DNA breaks: a focus on protein modifications. *Genes Dev* 25, 409–433.
- Potluri, V., Noothi, S.K., Vallabhapurapu, S.D., Yoon, S.O., Driscoll, J.J., Lawrie, C.H., and Vallabhapurapu, S. (2013). Transcriptional repression of Bim by a novel YY1-RelA complex is essential for the survival and growth of Multiple Myeloma. *PLoS ONE* 8, e66121.
- Redwood, A.B., Perkins, S.M., Vanderwaal, R.P., Feng, Z., Biehl, K.J., Gonzalez-Suarez, I., Morgado-Palacin, L., Shi, W., Sage, J., Roti-Roti, J.L., et al. (2011). A dual role for A-type lamins in DNA double-strand break repair. *Cell Cycle* 10, 2549–2560.
- Schmidt, J.C., and Cech, T.R. (2015). Human telomerase: biogenesis, trafficking, recruitment, and activation. *Genes Dev* 29, 1095–1105.
- Sedletska, Y., Giraud-Panis, M.J., and Malinge, J.M. (2005). Cisplatin is a DNA-damaging antitumour compound triggering multifactorial biochemical responses in cancer cells: importance of apoptotic pathways. *Curr Med Chem Anticancer Agents* 5, 251–265.
- Sfeir, A., and de Lange, T. (2012). Removal of shelterin reveals the telomere end-protection problem. *Science* 336, 593–597.

Shachar, S., Pegoraro, G., and Misteli, T. (2015). HIPMap: A High-Throughput Imaging Method for Mapping Spatial Gene Positions. *Cold Spring Harb Symp Quant Biol*.

Shay, J.W., and Bacchetti, S. (1997). A survey of telomerase activity in human cancer. *Eur J Cancer* 33, 787–791.

Shimi, T., Kittisopikul, M., Tran, J., Goldman, A.E., Adam, S.A., Zheng, Y., Jaqaman, K., and Goldman, R.D. (2015). Structural organization of nuclear lamins A, C, B1, and B2 revealed by superresolution microscopy. *Mol Biol Cell* 26, 4075–4086.

Singh, M., Hunt, C.R., Pandita, R.K., Kumar, R., Yang, C.R., Horikoshi, N., Bachoo, R., Serag, S., Story, M.D., Shay, J.W., et al. (2013). Lamin A/C depletion enhances DNA damage-induced stalled replication fork arrest. *Mol Cell Biol* 33, 1210–1222.

Soutoglou, E., Dorn, J.F., Sengupta, K., Jasin, M., Nussenzweig, A., Ried, T., Danuser, G., and Misteli, T. (2007). Positional stability of single double-strand breaks in mammalian cells. *Nat Cell Biol* 9, 675–682.

Swift, J., Ivanovska, I.L., Buxboim, A., Harada, T., Dingal, P.C., Pinter, J., Pajerowski, J.D., Spinler, K.R., Shin, J.W., Tewari, M., et al. (2013). Nuclear lamin-A scales with tissue stiffness and enhances matrix-directed differentiation. *Science* 341, 1240104.

Symington, L.S., and Gautier, J. (2011). Double-strand break end resection and repair pathway choice. *Annu Rev Genet* 45, 247–271.

Thompson, S.L., and Compton, D.A. (2008). Examining the link between chromosomal instability and aneuploidy in human cells. *J Cell Biol* 180, 665–672.

Vallabhapurapu, S., and Karin, M. (2009). Regulation and function of NF-kappaB transcription factors in the immune system. *Annu Rev Immunol* 27, 693–733.

Wallis, C.V., Sheerin, A.N., Green, M.H., Jones, C.J., Kipling, D., and Faragher, R.G. (2004). Fibroblast clones from patients with Hutchinson-Gilford progeria can senesce despite the presence of telomerase. *Exp Gerontol* 39, 461–467.

Wang, Z., Yi, J., Li, H., Deng, L.F., and Tang, X.M. (2000). [Extension of life-span of normal human fibroblasts by reconstitution of telomerase activity]. *Shi Yan Sheng Wu Xue Bao* 33, 129–140.

Wood, A.M., Rendtlew Danielsen, J.M., Lucas, C.A., Rice, E.L., Scalzo, D., Shimi, T., Goldman, R.D., Smith, E.D., Le Beau, M.M., and Kosak, S.T. (2014). TRF2 and lamin A/C interact to facilitate the functional organization of chromosome ends. *Nat Commun* 5, 5467.

Wu, G., Lee, W.H., and Chen, P.L. (2000). NBS1 and TRF1 colocalize at promyelocytic leukemia bodies during late S/G2 phases in immortalized telomerase-negative cells. Implication of NBS1 in alternative lengthening of telomeres. *J Biol Chem* 275, 30618–30622.

Xi, L., and Cech, T.R. (2014). Inventory of telomerase components in human cells reveals multiple subpopulations of hTR and hTERT. *Nucleic Acids Res* 42, 8565–8577.

Ye, J.Z., Donigian, J.R., van Overbeek, M., Loayza, D., Luo, Y., Krutchinsky, A.N., Chait, B.T., and de Lange, T. (2004). TIN2 binds TRF1 and TRF2 simultaneously and stabilizes the TRF2 complex on telomeres. *J Biol Chem* 279, 47264–47271.

Zhou, Y., and Paull, T.T. (2013). DNA-dependent protein kinase regulates DNA end resection in concert with Mre11-Rad50-Nbs1 (MRN) and ataxia telangiectasia-mutated (ATM). *J Biol Chem* 288, 37112–37125.